Accepted Manuscript

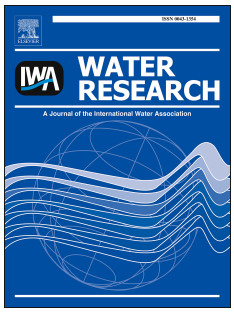

Towards reducing DBP formation potential of drinking water by favouring direct ozone over hydroxyl radical reactions during ozonation

Glen Andrew De Vera, Daniel Stalter, Wolfgang Gernjak, Howard S. Weinberg, Jurg Keller, Maria José Farré

PII: S0043-1354(15)30219-0

DOI: 10.1016/j.watres.2015.09.007

Reference: WR 11515

To appear in: *Water Research*

Received Date: 26 May 2015

Revised Date: 3 September 2015

Accepted Date: 4 September 2015

Please cite this article as: De Vera, G.A., Stalter, D., Gernjak, W., Weinberg, H.S., Keller, J., Farré, M.J., Towards reducing DBP formation potential of drinking water by favouring direct ozone over hydroxyl radical reactions during ozonation, *Water Research* (2015), doi: 10.1016/j.watres.2015.09.007.

Graphical abstract:

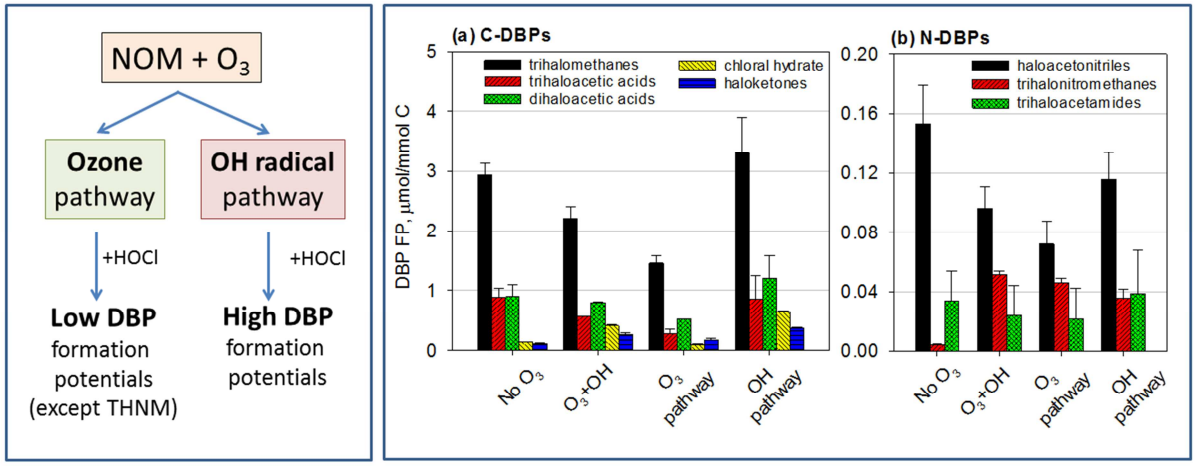

Towards reducing DBP formation potential of drinking water by favouring direct ozone over hydroxyl radical reactions during ozonation

Glen Andrew De Vera[*], Daniel Stalter[‡|], Wolfgang Gernjak[*§], Howard S. Weinberg[#], Jurg Keller[*], Maria José Farré[*§†]

[*]The University of Queensland, Advanced Water Management Centre, Queensland 4072, Australia

[‡]The University of Queensland, National Research Centre for Environmental Toxicology (Entox), Brisbane, Queensland 4108, Australia

[§]ICRA, Catalan Institute for Water Research, Scientific and Technological Park of the University of Girona, H_2O Building, Emili Grahit 101, 17003 Girona, Spain

[#]University of North Carolina at Chapel Hill, Department of Environmental Sciences and Engineering, 146A Rosenau Hall, Chapel Hill, North Carolina 27599, United States

[|]Swiss Federal Institute of Aquatic Science and Technology (EAWAG), Überlandstrasse 133, Dübendorf 8600, Switzerland.

[†]Corresponding author: Maria José Farré: phone: (+34) 972 18 33 80, email: mjfarre@icra.cat

Submitted to Water Research

Abstract

When ozonation is employed in advanced water treatment plants to produce drinking water, dissolved organic matter reacts with ozone (O_3) and/or hydroxyl radicals ($^{\bullet}OH$) affecting disinfection byproduct (DBP) formation with subsequently used chlorine-based disinfectants. This study presents the effects of varying exposures of O_3 and $^{\bullet}OH$ on DBP concentrations and their associated toxicity generated after subsequent chlorination. DBP formation potential tests and *in vitro* bioassays were conducted after batch ozonation experiments of coagulated surface water with and without addition of tertiary butanol (t-BuOH, 10 mM) and hydrogen peroxide (H_2O_2, 1 mg/mg O_3), and at different pH (6 – 8) and transferred ozone doses (0 – 1 mg/mg TOC).

Although ozonation led to a 24 – 37% decrease in formation of total trihalomethanes, haloacetic acids, haloacetonitriles, and trihaloacetamides, an increase in formation of total trihalonitromethanes, chloral hydrate, and haloketones was observed. This effect however was less pronounced for samples ozonated at conditions favoring molecular ozone (e.g., pH 6 and in the presence of t-BuOH) over $^{\bullet}OH$ reactions (e.g., pH 8 and in the presence of H_2O_2). Compared to ozonation only, addition of H_2O_2 consistently enhanced formation of all DBP groups (20 – 61%) except trihalonitromethanes. This proves that $^{\bullet}OH$-transformed organic matter is more susceptible to halogen incorporation. Analogously, adsorbable organic halogen (AOX) concentrations increased under conditions that favor $^{\bullet}OH$ reactions. The ratio of unknown to known AOX, however, was greater at conditions that promote direct O_3 reactions. Although significant correlation was found between AOX and genotoxicity with the p53 bioassay, toxicity tests using 4 *in vitro* bioassays showed relatively low absolute differences between various ozonation conditions.

Keywords: ozonation, hydroxyl radicals, disinfection byproducts, adsorbable organic halogens, in vitro bioassays

1. Introduction

Ozonation is used in many drinking water treatment plants because of its efficiency for disinfection as well as oxidation of micropollutants and natural organic matter (NOM) (Lee et al. 2013, von Gunten 2003a, Westerhoff et al. 1999). It has gained additional attention due to its potential to minimize formation of organic disinfection byproducts (DBPs) from subsequent chlorine disinfection. However, like other oxidants ozone has its own suite of DBPs including bromate in bromide-containing waters and other organic DBPs from partial oxidation of NOM (von Gunten 2003a). The latter is expected as typical ozonation conditions during drinking water treatment are insufficient for complete NOM mineralization (Nöthe et al. 2009, Ratpukdi et al. 2010, Zhang and Jian 2006). Since ozone is not used as a final disinfectant due to its short lifetime, it is commonly followed by chlorine or chloramines which can react with the remaining and structurally altered NOM to form additional byproducts.

Oxidation during ozonation involves reactions of molecular ozone (O_3) and/or hydroxyl radicals ($^{\bullet}OH$), the latter of which can be formed from ozone decomposition and reaction with NOM (Elovitz and von Gunten 1999) and is known to predominate at conditions that favor ozone decay (e.g., high pH or in presence of H_2O_2). Ozone decay, however, is slowed down at low pH or in the presence of $^{\bullet}OH$ reaction inhibitors such as tertiary butanol (Acero and von Gunten 2001, Elovitz et al. 2000). To describe the decay kinetics of ozone, the term exposure or its time-integrated concentration is commonly used, i.e., slower ozone decay corresponds to higher exposure and vice versa. Variations in concentrations of O_3 and $^{\bullet}OH$ may then result in different transformations of DBP precursors and are known to contribute to formation of bromate during multi-stage oxidation processes involving bromide, hypobromite, and oxybromine intermediates (von Gunten and Hoigné 1994). The presence of bromide can also affect the speciation of organic DBPs. Molecular ozone reacts via electrophilic addition directly and selectively with electron-rich functional groups such as unsaturated hydrocarbon bonds, activated aromatic systems, and non-protonated amines (Lee and von Gunten 2010, von

Gunten 2003b). ˙OH reactions involve more unselective and diffusion-controlled OH-addition and H-abstraction (von Gunten 2003b, von Sonntag 2008).

Apart from bromate, most studies in the literature have investigated the overall impact of the ozonation process on DBP formation without taking into consideration the influence of ˙OH reactions. Limited studies differentiated the effects of changing O_3 and ˙OH exposures especially on organic DBP formation. Singer et al. (1999) demonstrated that there was no consistent trend for the effect of ozonation pH on chlorination DBPs such as trihalomethanes (THMs), haloacetic acids (HAAs), dichloroacetonitrile (DCAN), trichloronitromethane (TCNM), and chloral hydrate (CH). However, Shan et al. (2012) showed an increase in halonitromethanes (HNMs) and THM formation at an ozonation pH of 8 compared to pH 6. Kleiser and Frimmel (2000) showed a less effective removal of THMs and adsorbable organic halogen (AOX) formation potentials in the ˙OH-dominant H_2O_2/UV process compared to ozonation. In addition, when O_3 and O_3/H_2O_2 processes were compared, Yang et al. (2012a) showed only a 5% variation in THM formation and an inconsistent trend in HAA and TCNM formation. The authors also observed an enhanced formation of haloacetonitriles (HANs), CH, and haloketones (HK) with O_3/H_2O_2 treatment followed by chlorination.

Despite these studies, it still remains ambiguous whether ozonation at conditions of higher O_3 or ˙OH exposures would improve removal of DBP precursors. Additional evidence is needed to confirm which oxidation pathway will assist water treatment plant operators in improving their control over regulated and emerging DBPs. Moreover, there is limited knowledge about the effect of oxidant dynamics during ozonation on formation of nitrogenous DBPs (N-DBPs) even though they are identified to be more toxic than their carbon-based DBP (C-DBPs) analogues (Plewa et al. 2008). Additionally, although ozonation before chlorination has been shown to reduce formation of the regulated THMs and HAAs (Hua and Reckhow 2013), it may potentially transform NOM into forms that render them capable of producing more toxic DBPs (Stalter et al. 2010) after chlorination. These effects may not be easily determined using conventional analytical techniques. For this purpose, recent studies have shown that chemical analysis of DBPs can be complemented with bioanalytical

tools such as *in vitro* bioassays to gain a better understanding of the transformations and toxicity that may occur after treatment (Farre et al. 2013, Lyon et al. 2014, Neale et al. 2012). These tools may also be useful in determining the effects of varying ozonation conditions on the quality of the final disinfected water.

This paper shows the effects of changing O_3 and $^{\bullet}OH$ exposures prior to chlorination on formation potentials of AOX, N-DBPs such as HANs, HNMs, and haloacetamides (HAMs) and the C-DBPs THMs, HAAs, CH, and HKs. *In vitro* bioassays were used to assess cytotoxicity, genotoxicity, and oxidative stress of the treated water. Thus, a holistic approach was applied to determine the overall impact of ozone and $^{\bullet}OH$ oxidation on the quality of water post-disinfected with chlorine in terms of known DBPs, AOX, and associated biological effects.

2. Experimental methods

2.1. Water sample

The settled water used in this study was representative of 9 sources with similar character treated at drinking water plants throughout South East Queensland (SEQ), Australia (Lyon et al. 2013) and was collected after coagulation and sedimentation from one of the plants. The treatment plant's source water originates from a catchment area (88 km^2) which introduces organic matter comprised mostly of allochthonous, plant- and soil-derived material. Across the 9 sources, total organic carbon (TOC) and specific UV absorbance (SUVA) were 3.9 ± 0.5 mg/L and 1.6 ± 0.1 L/mg-C·m, respectively. Differences in DBP formation potentials were also minimal (e.g., THMs and HANs had relative standard deviations of 22 and 30%, respectively) as shown in Figure S1. Thus, it is likely that the findings from study of this water would be applicable across the SEQ region.

To obtain a stock solution of organic matter that could be used for a series of ozonation experiments, the settled water was concentrated by reverse osmosis (RO) as described in Text S1. The characteristics of the source settled water and RO concentrate are shown in Table S1. The RO concentrate contained 181 ± 3 mg/L TOC, 6.0 mg/L total organic nitrogen, and 3.2 ± 0.1 mg/L

bromide. Iodide was below the reporting limit of 0.1 mg/L. To show that the concentration process did not significantly alter the characteristics of DBP precursors in the source settled water, volatile DBP formation potentials (in μmol/mmol C) of a reconstituted RO concentrate were compared to those in the settled water sample (Table S2).

2.2. Batch ozonation experiments

Experiments were performed as batch experiments mixing 1.2 μm GF/C (Whatman, UK) filtered reconstituted RO concentrate with ozone stock solutions. Reconstituted water was prepared by mixing deionized water (MilliQ A10 Advantage, Millipore, Australia) with RO concentrate to a TOC concentration of 17 ± 2 mg/L, a level that helped to improve detection of all targeted DBPs. The samples were buffered with 1 mM phosphate to ensure relatively constant pH (± 0.2 pH units) during ozonation. All ozonation experiments were carried out in triplicate and results are reported as mean ± standard deviation. For this study, the following baseline conditions were defined: transferred ozone dose = 0.75 mg/mg TOC, inorganic carbon concentration = 0 mg/mg TOC, pH = 7, temperature = 22°C and bromide concentration = 20 μg Br^-/mg TOC. Details on preparation of ozone stock solutions (1 – 1.5 mM O_3) are discussed in Text S2.

The first set of batch ozonation experiments used samples with and without added tertiary butanol (t-BuOH; 10 mM; Sigma-Aldrich, 99.6%, St. Louis, MO, USA) and hydrogen peroxide (H_2O_2; 15 mg O_3/L; Merck, 30%, Darmstadt, Germany) to distinguish the effects of direct O_3 and $^{\bullet}OH$ reactions on DBP formation. To confirm these results, the second set studied the effect of varying pH levels (6, 7, 8) on ozonation using samples buffered with 1 mM phosphate ($NaH_2PO_4 \cdot 2H_2O$ (>99%, Ajax Finechem, NSW, Australia) and $Na_2HPO_4 \cdot 2H_2O$ (≥99.5%, Merck, Darmstadt, Germany)). The third set varied transferred ozone dose (0, 0.4, 0.75, 1 mg/mg TOC) to determine the impact of having both O_3 and $^{\bullet}OH$ reactions on DBP formation. Ozone doses were adjusted in each experiment to simulate actual O_3/TOC ratios of water utilities in SEQ. After all the ozone had reacted, samples were stored headspace free at 4°C for no more than 24 hours until conducting DBP formation potential tests. Characterization methods for TOC, absorbance, fluorescence, aldehyde, and inorganic nitrogen

content are discussed in Text S3. Experiments without ozone addition were also conducted with the same TOC, inorganic carbon, bromide, and pH as the baseline conditions. Samples for bromate analysis were collected before DBP formation potential tests.

2.3. Formation potential tests

Formation potential tests were carried out in 250 mL headspace-free samples buffered at pH 7 with 10 mM phosphate. The buffer was prepared from a mixture of KH_2PO_4 (99%) and NaOH (98%) both purchased from Chem-Supply, SA, Australia. The concentration of sodium hypochlorite (reagent grade, available chlorine 4 − 4.99%, Sigma-Aldrich, St. Louis, MO, USA) added was based on chlorine demand tests with the same water and aimed to have a residual of 1 – 2 mg/L as Cl_2 after 24 h to simulate realistic conditions. Prior to this, residual H_2O_2 for samples treated with O_3/H_2O_2 was quenched using either equimolar concentrations of sodium sulfite (≥98%, Sigma-Aldrich, Japan) or excess sodium hypochlorite (Liu et al. 2003). The latter was used simultaneously for quenching H_2O_2 and the excess for DBP formation potential tests. Chlorine residual in samples was measured using the *N*,*N*-diethyl-*p*-phenylenediamine (DPD) free chlorine colorimetric method (Hach, Loveland, CO, USA). After one day of contact time, samples were quenched of chlorine depending on the subsequent analytical fraction (i.e. L-ascorbic acid (≥99%, Sigma-Aldrich, China), sodium sulfite (≥98%, Sigma-Aldrich, Japan), and ammonium chloride (99.5%, Sigma-Aldrich, Japan) prior to extraction of neutral-extractable DBPs, AOX, and haloacetic acids, respectively). DBP formation potentials were normalized to the measured TOC of the water samples before ozonation and reported in μmol/mmol TOC to account for possible variability in preparing reconstituted water samples. For bioassays, 500 mL of ozonated samples were also subjected to 24-h formation potential tests with chlorine. The residual chlorine was quenched with equimolar concentrations of sodium thiosulfate ($Na_2S_2O_3 \cdot 5H_2O$; 99.5%, Sigma-Aldrich, USA) as described by Farré et al. 2013 and Yeh et al. 2014.

2.4. Analysis of disinfection by-products

The neutral extractable volatile DBPs analyzed for all samples included four trihalomethanes (THM4; trichloromethane (TCM), tribromomethane (TBM), bromodichloromethane (BDCM), and

dibromochloromethane (DBCM)), chloral hydrate (CH), two haloketones (HK; 1,1-dichloropropanone (1,1-DCP) and 1,1,1-trichloropropanone (1,1,1-TCP)), four haloacetonitriles (HAN4; trichloroacetonitrile (TCAN), dichloroacetonitrile (DCAN), bromochloroacetonitrile (BCAN), and dibromoacetonitrile (DBAN)), two trihalonitromethanes (THNM; trichloronitromethane (TCNM) and tribromonitromethane (TBNM)), and three trihaloacetamides (THAM; trichloroacetamide (TCAM), bromodichloroacetamide (BDCAM), and dibromochloroacetamide (DBCAM)). Other HAMs and iodinated DBPs were also measured but their concentrations were below their method reporting limits. The standards were purchased from different suppliers as specified in Text S4. As described by Farré et al. (2013), each sample was extracted in duplicate with methyl tert-butyl ether (MtBE; 99.9%, Sigma-Aldrich, St. Louis, MO, USA) and analyzed using an Agilent 7890A gas chromatograph with electron capture detector (GC/ECD) (Agilent, Shanghai, China) that has a dual injection (two injectors/columns/detectors on the same GC/ECD). The method reporting limit for volatile DBPs was 0.1 μg/L with recoveries normally ranging from 70% to 120%.

The haloacetic acids (HAAs) were classified into (i) trihaloacetic acids (THAAs) which included trichloroacetic acid (TCAA), bromodichloroacetic acid (BDCAA), and chlorodibromoacetic acid (CDBAA), and (ii) dihaloacetic acids (DHAAs) which included dichloroacetic acid (DCAA), bromochloroacetic acid (BCAA), and dibromoacetic acid (DBAA). These together with monochloroacetic acid (MCAA) and monobromoacetic acid (MBAA) were measured at Queensland Health Scientific and Forensic Services (QHFSS) based on EPA Method 552.3 (Domino et al. 2003) using an acidic, salted microextraction followed by derivatization with acidic methanol and GC/ECD analysis (Xie et al. 2002). The method reporting limit for all HAA species was 5 μg/L. Tribromoacetic acid was not analyzed because of its low stability during extraction with MtBE.

The analysis of adsorbable organic halogen (AOX) was based on previously reported methodologies (Farré et al. 2013, Yeh et al. 2014). This involves carbon adsorption and pyrolysis measurement on a Mitsubishi AQF-2100 Automated Quick Furnace unit followed by a Dionex ICS-2100 dual channel ion chromatograph system (Thermo Fisher Scientific, Australia).

Bromide, iodide, and bromate were measured at QHFSS using a Metrohm 861 (Herisau, Switzerland) Advanced Compact ion chromatograph equipped with Thermo AS23 and AG23 columns and a 50 μL sample loop. The eluent (0.477 g/L sodium carbonate and 0.067 g/L sodium bicarbonate in MilliQ water) flow rate was 1 mL/min and its conductivity suppressed using Metrohm's chemical (100 mM H_2SO_4) and CO_2 suppression modules. The reporting limits for bromide, iodide, and bromate were 0.005, 0.1, and 0.01, mg/L, respectively.

2.5. Sample preparation for bioassays

The quenched chlorinated 500 mL samples were first acidified to pH 1.5 using sulfuric acid (98%, Merck, Darmstadt, Germany) followed by a solid phase extraction (SPE) using TELOS ENV 1g/6ml cartridges (Kinesis, QLD, Australia). It should be noted that samples used here (TOC = 19 mg/L) were already enriched 4 times compared to TOC of actual water samples (4.8 mg/L). The cartridges were conditioned with 20 mL each of MtBE, methanol (≥99.8%, Merck, Darmstadt, Germany), and MilliQ water adjusted to pH 1.5 with sulfuric acid, respectively. After sample loading, cartridges were dried with >99.998% nitrogen gas. The retained compounds were eluted with 20 mL methanol followed by 20 mL MtBE. The eluates were blown down to 200 μL, which generates a 2,500 concentration factor for those DBPs completely recovered through the process. This extraction procedure enriched only non-volatile DBPs while the more volatile compounds were likely lost during the blow-down step (Neale et al. 2012). With the initial ~4-fold enrichment of TOC, the effects of treatment on the original settled water were highly magnified to the point of making any differences in biological effect more discernible. Extracts were stored at -80 °C and analyzed within 4 weeks.

2.6. Bioassays

Four types of *in vitro* bioassays were used to target nonspecific and reactive endpoints. These together with the relevant reference compounds were the bacterial cytotoxicity (Microtox) or bioluminescence inhibition assay with *V. fischeri* using phenol (Tang et al. 2013), the umuC bacterial reporter gene assay for genotoxicity using 4-nitroquinoline-1-oxide (Reifferscheid et al. 1991), the AREc32 MCF7 human cell reporter gene assay for oxidative stress using t-butylhydroquinone (tBHQ)

(Escher et al. 2012), and the p53RE-bla HCT-116 human cell reporter gene assay for genotoxicity using benzo(a)pyrene (Yeh et al. 2014). 1% methanol was used as negative control in the assay medium. Relative enrichment factors (REF) were calculated from the ratio of a 10,000 enrichment factor of sample (representing the combination of 4-fold TOC enrichment and 2,500 concentration factor by SPE) to the bioassay dilution factor (i.e., dilution of SPE extracts with assay medium by factor of 100). Each sample was analyzed in an 8-point serial dilution. For Microtox, the 50% effect concentration (EC_{50}) was derived from a log-logistic concentration-effect curve and corresponds to an REF which induces 50% of the maximum effect. For other bioassays, effect concentration (EC) is defined as induction ratio (IR) of 1.5 ($EC_{IR1.5}$) which corresponds to the REF needed to elicit 1.5 times induction of effect (e.g., production of luciferase for the AREc32 assay) compared to the negative control. Thus, water samples that have lower ECs are more toxic. The contribution of t-BuOH to toxicity was not measured since it is expected to have been lost during SPE. Further details on the bioassays were reported previously (Farré et al. 2013, Neale et al. 2012, Yeh et al. 2014).

3. Results and Discussion

3.1. Effect of ozonation conditions on formation of known DBPs

Figure 1 compares DBP formation potential of samples collected for three replicate experiments with and without previous ozonation at a dose of 0.75 mg O_3/mg TOC and pH 7 (columns labelled as "O_3" and "No O_3"). As expected, ozone increased the formation potentials of CH, HKs, and THNMs (Bond et al. 2011, Krasner 2009, Singer et al. 1999, Yang et al. 2012a) by 192%, 133%, and 1079%, respectively. The average concentration of other DBPs decreased in the following order: HAN4 (37%) ≈ THAA (37%) > THAMs (28%) ≈ THM4 (25%) > DHAAs (11%). Iodinated DBPs (I-DBPs) were all below detection limits which is in agreement with the study of Allard et al. (2013) which showed ozonation of iodide to iodate preventing I-DBP formation.

Differences in DBP formation are dependent on precursor characteristics and their reactivity towards O_3. When ozone reacts with nitrogen-containing moieties such as amines, R-NO_2 products are

formed which are THNM precursors (Bond et al. 2014) but these remove the nitrogen source for HAN4 and THAM formation explaining the observed trends in these experiments. Moreover, an increase in in NO_3^--N concentrations (7.6 – 44.5 μg/L) was observed, indicating direct attack of ozone on the nitrogen atom yielding a mixture of products including nitroalkanes and nitrate, among others. Ozonation of C-DBP precursors (e.g., phenol-type entities), on the other hand, occurs via a Criegee-type reaction where aromatic rings are cleaved forming muconic-type and aliphatic products (Wenk et al. 2013) including precursors of CH and HKs. This is reflected in a measured decrease in SUVA from 1.88 L/mg-C·m in the source water down to 0.88 L/mg-C·m after ozonation at 0.75 mg O_3/mg TOC (Figure S2a). At this same ozone dose, an 80% decrease in fluorescence intensities of humic and fulvic acid-like peaks was also observed (Figure S2b). During this process, electron-rich constituents of NOM are oxidized leading to fewer halogenation sites (Westerhoff et al. 2004) that are necessary for THM and HAA precursors. The oxidized NOM also becomes more hydrophilic resulting in a large decrease in THAAs whose precursors are known to be more hydrophobic compared to those of THMs and DHAAs (Hua and Reckhow 2007). This increase in hydrophilicity also enhanced formation of bromine-containing DBPs such as DBCM, TBM, DBAA, CDBAA, DBAN, TBNM, and DBCM (Table S3) from oxidation by both O_3 and $^{\bullet}OH$. The influence of each oxidant on DBP formation was then distinguished by addition of t-BuOH and H_2O_2 to represent O_3-and $^{\bullet}OH$-dominant conditions, respectively.

3.1.1. Addition of tertiary butanol and H_2O_2

Figure 1 shows that ozonation of water samples in the presence of t-BuOH decreased the formation potentials of both C- and N-DBPs compared to O_3 with H_2O_2 and O_3 alone, the latter containing a mixture of molecular ozone and $^{\bullet}OH$. The results confirm that reactions of molecular ozone decreased nucleophilic centers of NOM available for chlorine substitution (Westerhoff et al. 2004). They also support the observations of Wenk et al. (2013) that direct O_3 reactions resulted in NOM with lower electron-donating capacity compared to non-selective oxidation with $^{\bullet}OH$.

The average formation potentials of each DBP species are presented in Table S3. It should be noted that in the presence of NOM, t-BuOH is less likely to react with molecular ozone ($k = 3x10^{-3}$ $M^{-1}s^{-1}$) (Reisz et al. 2014). This was apparent from lower DBP formation potentials produced from samples treated with O_3/t-BuOH compared to O_3 only and O_3/H_2O_2. Control experiments using ozonated t-BuOH in pure water were performed to investigate DBP formation related to t-BuOH. In pure water, TCM and AOX concentrations produced from ozonated t-BuOH were only about 15% of the formation potentials observed for water samples treated with O_3/t-BuOH. In the presence of NOM, this percentage is expected to be much lower. Ozonation of t-BuOH alone, however, may form acetone and butan-2-one (Reisz et al. 2014) and $^{\bullet}OH$ scavenging may form formaldehyde (Nöthe et al. 2009). These compounds can possibly act as precursors of HKs including 1,1,1-TCP and 1,1-DCP whose respective concentrations after ozonation of t-BuOH in pure water were 72% and 21% higher than the formation potentials of water samples treated with O_3/t-BuOH. As can be seen from Figure 1, this possible increase in DBP formation potentials was not apparent in the actual water sample due to competing reactions with more reactive NOM, producing less HKs compared to O_3 only and O_3/H_2O_2 conditions. This strongly suggests that t-BuOH does not contribute to further DBP formation in our water sample.

In terms of THM4, addition of t-BuOH caused a further 34% decrease in their formation potential compared to ozonation without t-BuOH. This implies that t-BuOH improved the reaction of O_3 towards THM precursors which are often correlated with hydrophobic fractions containing aromatic carbon and this is reflected in decreased fluorescence at the humic and fulvic acid-like regions (Figure S3). When O_3/H_2O_2 was used, THM4 formation potentials after subsequent chlorination increased by 50% relative to O_3 only and were almost equal to those in samples without O_3. Such an increase is consistent with the increased SUVA and fluorescence observed in O_3/H_2O_2 treatments compared to ozone alone (Figures S2a and b).

The results for HAAs were similar to those observed for THM4. Relative to ozonated samples without H_2O_2, THAA and DHAA formation potentials were higher by about 50% after O_3/H_2O_2

treatment. On the other hand, addition of t-BuOH during ozonation lowered THAA and DHAA formation potentials by 50% and 35%, respectively. These findings are reflected in the decrease for chlorine demand when O_3 reactions were favored over $^{\bullet}OH$ reactions (Figure S2c). For example, ozonated samples without t-BuOH had a chlorine demand of 12.3 mg/L while this value was reduced to 10.1 mg/L in those ozonated samples to which t-BuOH was added.

Although the levels of CH and HKs after chlorination increased with ozonation as a result of increased aldehyde and methyl ketone species, their formation potentials were still lower with O_3/t-BuOH (CH=0.09; HK=0.17 μmol/mmol C) than those treated with O_3/H_2O_2 (CH=0.64; HK=0.36 μmol/mmol C). In the presence of t-BuOH, CH decreased by 79% and HKs by 35% compared to samples ozonated without t-BuOH. These findings suggest that $^{\bullet}OH$ radicals are able to react with O_3-refractory moieties of NOM leading to formation of more CH and HK precursors. This is demonstrated in lower acetaldehyde concentrations measured after ozonation in the presence of t-BuOH than with H_2O_2 (Figure S4).

The observed trends for THM4, HAAs, CH, and HKs also occurred for N-DBPs pertaining to the groups of HAN4 and THAMs. The formation potentials of HAN4 were reduced by 53% in the presence of t-BuOH while in presence of H_2O_2, the reduction was 29% lower. The results shown here were consistent with the findings of Molnar et al. (2012a) who showed that $^{\bullet}OH$ reactions generated from TiO_2-catalyzed ozonation resulted in an increase in hydrophilic NOM fractions, which are known to contain HAN precursors. In terms of THAMs, which can be formed from hydrolysis of HANs (Glezer et al. 1999) or from other HAN-independent reactions (Huang et al. 2012), addition of t-BuOH tends to improve reduction of THAM formation potentials relative to ozonation without t-BuOH. With O_3/H_2O_2, the formation potentials were even higher compared to samples not treated with ozone. The differences between these treatments, however, showed weak statistical significance due to large deviations arising from relatively low THAM concentrations.

The differences between THNM formation potentials (sum of TCNM and TBNM) in samples treated with and without t-BuOH and H_2O_2 were not markedly significant ($p=0.06$) due to contrasting

changes in concentrations of TCNM and TBNM (Table S3). TCNM concentrations were lower in ozonated samples with either t-BuOH or H_2O_2. At these conditions, a rupture of the C – N bond to form inorganic nitrogen is likely such that HNM formation is minimized regardless of whether the reaction proceeds via the O_3 or $^{\bullet}OH$ pathways. This mechanism is supported by previous studies where reactions of O_3 and $^{\bullet}OH$ with organic nitrogen were observed to yield nitrate and ammonia as end products, respectively (Berger et al. 1999, Le Lacheur and Glaze 1996). The results here also demonstrate that not only O_3 but also $^{\bullet}OH$ may form nitroalkane groups (Shah and Mitch 2012) through formation of more oxidizing radical species from ozone decomposition (e.g., $O^{\bullet-}$) as proposed by Shan et al. (2012). Significant differences were observed for TBNM ($p<0.05$). Compared to ozonation alone and in the presence of H_2O_2, TBNM formation potential was higher for ozonated samples containing t-BuOH. This is a result of an increased $HOBr/OBr^-$ concentration, which enhances bromine substitution into nitroalkane groups. The changes in percent bromine substitution factors after ozonation are illustrated in Figure S5. These values were calculated from the ratio of the molar concentration of bromine incorporated in one DBP group to the total molar concentration of chlorine and bromine in that group (Hua and Reckhow 2013). Less TBNM was found in samples containing H_2O_2 most likely due to the reduction of $HOBr/OBr^-$ to Br^- by H_2O_2 as reported by von Gunten and Oliveras (1998). Similar trends were observed for other bromine-containing DBPs including DBCM, TBM, DBAN, TBNM, DBCAM, DBAA, and CDBAA.

3.1.2. Ozonation pH

The changes in formation potentials with varying ozone and $^{\bullet}OH$ exposures were confirmed using ozonation conditions at different pH. Consistent with our earlier results, formation potentials of C-DBPs were found to be lower at pH 6 where the molecular ozone pathway predominates compared to pH 8 (Figure 2).

Compared to chlorination of non-ozonated samples, THM4 formation potentials decreased by 35% when samples ozonated at pH 6 were subsequently chlorinated to achieve the same target residual. When ozonation was carried out at pH 8, THM4 formation potential was 20% higher than at pH 6.

This could be the result of increased $^{\bullet}$OH reaction with aromatic structures in NOM making it more susceptible to halogenation with chlorine (Kleiser and Frimmel 2000, von Gunten 2003a). Kleiser and Frimmel (2000) also proposed that $^{\bullet}$OH attack on NOM via H-abstraction of aliphatic structures and reactions with oxygen and peroxyl radicals may produce alcohol or keto-groups which react with chlorine to form THMs (Kleiser and Frimmel 2000).

A similar trend was observed for HAAs but with a higher increase at pH 8 for DHAAs (31%) compared to THAAs (21%). This difference could be related to the change in content and structure of HAA precursors. At higher ozonation pH, more hydrophilic NOM fractions could form which are known precursors of DHAA. In a study by Molnar et al. (2012b), 3 mg O_3/mg DOC ozonation of a raw water sample at pH 10 compared to pH 6 increased the hydrophilic NOM fraction to 90%. This fraction may contain β-dicarbonyl acid species which are important in DHAA formation (Bond et al. 2009).

The degradation products of $^{\bullet}$OH reactions with NOM (e.g., saturated compounds like aldehydes and ketones) are also important for formation of CH and HK as shown in the previous section. The formation potentials of these groups increased after ozonation with this increase being stronger at pH 8 compared to lower pH. This provides further evidence that a shift from O_3 to $^{\bullet}$OH radical pathways promotes formation of precursors of halogenated aldehydes (Figure S4) and ketones.

After ozonation, HAN4 and THAM formation potentials decreased with concurrent increase in THNM formation potential. However, across the ozonation pH levels used in this study, no significant differences were observed for the N-DBPs analyzed. This could mean that at these conditions, O_3 and $^{\bullet}$OH, despite their having different concentrations, are able to react with organic nitrogen leading to similar N-DBP precursor concentrations before chlorination. The results may also imply that the change in O_3 and $^{\bullet}$OH exposures at the pH used may be insufficient to cause dramatic change in precursor concentrations as compared to exposures obtained through addition of t-BuOH and H_2O_2, as demonstrated in the previous section. This may also have an implication on the nature of organic nitrogen present in the sample. Shan et al. (2012), for example, showed that most amino acids (except

388 glycine and lysine) and amino sugars did not cause an apparent increase in the yield of HNMs when
389 ozonation pH was increased from pH 6 to 8.

390 *3.1.3. Transferred ozone dose*

391 Figure 3 shows the effect of increasing ozone dose on formation potentials of C- and N-DBPs. It
392 should be noted, however, that increasing ozone dose may not completely differentiate the effects of
393 ozone and •OH because, as shown in Figure S6, the exposures of both oxidants increase with dose.
394 Thus, this section demonstrates the combined effects of ozone and •OH on formation potentials of
395 DBPs.

396 Ozonation at an initial low transferred dose of 0.4 mg/mg TOC led to 20 – 40% lower formation of
397 THM4, THAAs, DHAAs, HAN4, and THAMs after chlorination compared to non-ozonated samples
398 that were chlorinated to achieve the same target residual. When the ozone dose was increased, no
399 statistically significant effect was observed for THM4. This could be a result of competing effects of
400 O_3 and •OH reactions, (i.e., molecular O_3 reactions minimize THM formation while •OH reactions
401 form more precursors). Although bromine-containing THMs increased after ozonation, only slight
402 variations in their formation potentials were observed when ozone dose was increased (Table S3).

403 HAA precursor concentrations were also reduced during initial low dose ozonation. However, at
404 higher ozone doses, THAA and DHAA formation potentials appeared to increase slightly. From 0.4 to
405 1 mg O_3/mg TOC, concentrations of THAAs increased by 15% while those of DHAAs increased by
406 22%. Between the two groups and at all ozone doses, THAA formation potentials were lower than
407 those of DHAAs because of the more hydrophobic nature of the former (Hua and Reckhow 2007).
408 The same rationale applies for higher reduction of THAA formation potentials at the same 0.75 mg
409 O_3/mg TOC ozone dose (37%) compared to THM4 (25%).

410 The formation potentials of CH and HK were shown to increase at higher ozone doses. Compared
411 to samples without ozone, CH and HK increased by 137 to 209% and 64 to 190% from 0.4 to 1 mg
412 O_3/mg TOC, respectively. These results demonstrate that despite having high ozone exposure, the
413 strong contribution of •OH in the formation of aldehydes and methyl ketone precursors resulted in an

414 increase in CH and HK formation. The increases in aldehyde concentrations are presented in Figure
415 S7. These results, together with those observed at different ozonation pH, show that ozonation at
416 lower doses and pH may be necessary for better control of C-DBP formation.

417 Ozonation of dissolved organic nitrogen with increasing dose may result in a mixture of oxidized
418 amines, nitriles, and amides. The formation potentials of HAN4 and THAMs decreased 30 to 41% and
419 20 to 32%, respectively, when ozone dose increased from 0.4 to 1 mg O_3/mg TOC. Although the
420 differences in concentrations after ozonation did not reach statistical significance ($p>0.05$), the
421 decreasing trend in formation potentials at higher ozone dose suggests favorable oxidation of HAN4
422 and THAM precursors to nitroalkane groups which in turn promotes THNM formation (Huang et al.
423 2012, Yang et al. 2012b). These reactions may explain the significant increase in THNM formation
424 potentials from 0.005 to 0.060 μmol/mmol C when ozone dose was increased.

425 Since bromate, formed during ozonation, is among the DBPs of most interest, it was also
426 measured after ozonation at different conditions. Both direct O_3 and $^{\bullet}OH$ radical reaction pathways
427 were reported to significantly affect bromate formation through mechanisms involving oxidation of
428 bromide and bromite by molecular O_3 and oxidation of intermediate oxybromine species by $^{\bullet}OH$ (von
429 Gunten and Hoigné 1994). Figure S8 shows bromate concentrations during ozonation at various
430 transferred ozone doses, bromide and inorganic carbon concentrations, and in the presence of t-BuOH
431 and H_2O_2. Bromate increased with increasing ozone dose and bromide concentrations. When
432 inorganic carbon was increased from 0 to 6 mg/mg TOC at the same ozone dose (0.75 mg/mg TOC)
433 and bromide concentration (20 μg/mg TOC), bromate increased from 0.01 to 0.05 mg/L due to
434 reactions of bromide and hypobromite with molecular ozone, $^{\bullet}OH$, and carbonate radicals formed
435 from $^{\bullet}OH$ scavenging by HCO_3^-/CO_3^{2-} (von Gunten and Hoigné 1994). In natural waters, a higher
436 inorganic carbon can elevate pH which might favor bromate formation by the $^{\bullet}OH$ pathway. In the
437 presence of t-BuOH and H_2O_2 at 0.75 mg O_3/mg TOC and the same bromide concentration (20 μg/mg
438 TOC), no bromate was formed which is similar to the observations of Gillogly et al. (2001). H_2O_2
439 reduces HOBr to Br^- while t-BuOH can scavenge available $^{\bullet}OH$. Since no bromate was found after

ozonation with t-BuOH, the •OH pathway, therefore, played an important role in bromate formation in our water samples. It should be noted that the reported bromate concentrations in our study came from reconstituted water samples (TOC = 18 mg/L) which are about 4 to 10 times more concentrated than commonly encountered in water treatment plants where the resulting bromate concentrations would typically be much lower.

3.2. Effect of ozonation conditions on formation of unknown byproducts

One of the concerns during ozonation is the formation of unknown transformation products that may be associated with certain toxic effects. To address this, AOX and *in vitro* bioassays were conducted after the ozonated water had been chlorinated in the formation potential tests.

Figure 4a shows the changes in AOX at different ozonation conditions which could be partially attributed to the largest constituents (THM4 at 29 – 42% and total HAAs at 16 – 22% across all experimental conditions in this study). The results were generally consistent with those observed for the sum of the measured DBPs, i.e., conditions that favor molecular ozone over •OH reactions led to lower AOX formation potentials. Figure S9 shows examples of changes in AOX distributions as a function of different oxidant exposure. After chlorination of O_3/t-BuOH treated water, the AOX concentration (12.1 μmol/mmol C) was found to be lower than AOX from ozonation at ambient conditions (20.5 μmol/mmol C). Higher AOX was found for O_3/H_2O_2 treatment (25.0 μmol/mmol C) which was 11% higher than AOX from samples not treated with ozone. AOX at pH 8 (21.4 μmol/mmol C) was also higher than AOX at pH 6 (18.0 μmol/mmol C). AOX formation potentials also had an initial decrease of 30% at 0.4 mg O_3/mg TOC followed by an increase in concentrations in the range of 15.7 – 23.3 μmol/mmol C with increasing ozone dose. This supports our hypothesis that the increase in DBP formation potentials with ozone dose is due to •OH induced formation of halogen reactive organic matter fractions. This can be seen from a linear relation of AOX formation potentials with chlorine demand of samples ozonated at different conditions (Figure S10).

Another notable outcome of ozonation at different O_3 exposures is the change in unknown to known AOX ratio (UAOX/AOX) (Figure 4b). UAOX refers to the difference between the measured

AOX and the organic halogen content of the measured DBPs. It was clearly shown that conditions that promote molecular ozone reactions have higher UAOX/AOX values compared to conditions that promote $^{\bullet}OH$ reactions. For example, samples ozonated with t-BuOH had a UAOX/AOX value of 50% while those treated with O_3/H_2O_2 only had 27%. Ozonation at pH 6 resulted in a UAOX/AOX value of 60% while at pH 8, this ratio decreased to 52%. The gap between the total AOX and known AOX became closer when the %AOX accounted for by the measured THMs and HAAs was higher (Figure S11).

The changes in reactivity of the organic matter towards chlorine after ozonation may also influence the overall toxicity of the treated water sample. A summary of the bioassay responses are presented in Figure 5. Symbols E1 – E6 correspond to the toxicity and AOX data of 6 ozonation experiments at different pH (6 and 8) and ozone dose (0, 0.4, 0.75 and 1 mg/mg TOC). The points for O_3/t-BuOH and O_3/H_2O_2 were not included in the linear regression so as to have responses from water samples with relatively constant characteristics. Among the bioassays, the p53 assay was the only test to show a significant correlation between AOX and genotoxicity ($p = 0.006$; $R^2 = 0.87$), i.e., the higher the AOX, the more genotoxic the water becomes. Since less AOX was produced when conditions favored direct ozone reactions, it also follows that genotoxicity could be lower at similar conditions. Other than non-volatile DBPs, genotoxicants causing the response may also include other oxidation products such as aldehydes and aldehyde-containing moieties which may potentially damage DNA and enzymes (Magdeburg et al. 2014, Petala et al. 2008).

Despite the correlation found for the p53 assay, the differences in toxic response from the other bioassays were generally less pronounced. The toxicity of all O_3/HOCl treated waters in our study remained relatively constant and within the commonly encountered precision of bioassay responses despite observed changes of AOX concentration with varying oxidant exposures. This suggests that the toxicological impact of AOX generated by a combination of ozone and chlorine compared to chlorine alone is insignificant. This is in contrast to studies evaluating other water treatment combinations (Farré et al. 2013, Reungoat et al. 2010). The study of Farré et al. (2013), for example,

showed less variability in toxicity between samples treated with HOCl and NH_2Cl. When source waters with different organic matter characteristics and concentrations were used (e.g., samples from conventional drinking water treatment plant and a desalination plant), large differences in effect concentrations were observed. Hence, neither organic matter changes nor DBP formation brought about by different ozone exposures is sufficient to elicit a statistically significant trend in toxicity or the toxicity assays used in this study are not as sensitive as AOX measurements when it comes to evaluating ozonation effects on organic matter transformation.

4. Conclusions

This study evaluated the effects of ozonation conditions on formation potentials of C-DBPs, N-DBPs, AOX, and associated toxicity after chlorine disinfection. From this study, the following conclusions can be drawn:

- Ozonation at conditions favoring molecular ozone over the $^{\bullet}OH$ pathway promotes reduction of halogenated DBP formation potentials with subsequent chlorination. This observation also applies to DBPs that are known to form as a result of pre-ozonation and subsequent chlorination such as CH and HKs. Table S4 provides a summary of percent removals of DBP formation potentials during ozonation under direct ozone- and $^{\bullet}OH$-dominant conditions.
- Increasing ozone dose without changing other conditions (e.g., pH, no addition of t-BuOH or H_2O_2) resulted in a mixture of effects brought about by additional O_3 and $^{\bullet}OH$ reactions. DBP formation potentials first decreased at the initial O_3 dose but increased at higher doses due to the contribution of $^{\bullet}OH$ in organic matter oxidation once it was no longer susceptible to direct reactions with ozone.
- The results for AOX followed the trend for known DBPs analyzed. Subjecting samples to conditions favoring ozone reaction pathway resulted in lower AOX formation potentials but a higher percentage of UAOX.

- *In vitro* bioassay results for p53 showed significant correlation with AOX formation. Although the toxic effects were not very prominent in this study, the observed differences imply that the degree of oxidation prior to chlorine disinfection could influence the overall toxicity of the treated water. No significant changes in toxicity were observed using Microtox, umuC and AREc32 bioassays.

Acknowledgements

This study was funded by a tailored collaboration with Seqwater (Australia) and the Water Research Foundation (project WRF #4484). Glen De Vera is grateful for the Australia Awards PhD scholarship. Dr. Maria José Farré acknowledges the European Commission for funding project 623711 under the FP7-PEOPLE-2013-IIF - Marie Curie Action: "International Incoming Fellowships" and Dr Wolfgang Gernjak acknowledges funding obtained from the Spanish Government for a Ramon y Cajal Research Fellowship (RYC-2012-12181). Dr. Daniel Stalter would like to acknowledge funding through a Marie Curie International Outgoing Fellowship within the 7th European Community Framework Program (PIOF-GA-2012-329169). Elissa O'Malley is acknowledged for her contributions on the bioanalytical analysis of the water samples. The authors would also like to thank Deb Gale and other Seqwater staff who were involved in the sampling at treatment plants.

References

Acero, J. and von Gunten, U. (2001) Characterization of oxidation processes: Ozonation and the AOP O_3/H_2O_2. J. Am. Water Works Ass. 93(10), 90-100.

Allard, S., Taylor, C.E., Chan, W.M., Joll, C.A. and von Gunten, U. (2013) Ozonation of iodide-containing waters: selective oxidation of iodide to iodate with simultaneous minimization of bromate and I-THMs. Water Res. 47(3), 1953-1960.

Berger, P., Karpel Vel Leitner, N., Dore, M. and Legube, B. (1999) Ozone and hydroxyl radicals induced oxidation of glycine. Water Res. 33(2), 433-441.

543 Bond, T., Goslan, E.H., Jefferson, B., Roddick, F., Fan, L. and Parsons, S.A. (2009) Chemical and
544 biological oxidation of NOM surrogates and effect on HAA formation. Water Res. 43(10), 2615-
545 2622.
546 Bond, T., Huang, J., Templeton, M.R. and Graham, N. (2011) Occurrence and control of nitrogenous
547 disinfection by-products in drinking water--a review. Water Res. 45(15), 4341-4354.
548 Bond, T., Templeton, M.R., Rifai, O., Ali, H. and Graham, N.J. (2014) Chlorinated and nitrogenous
549 disinfection by-product formation from ozonation and post-chlorination of natural organic matter
550 surrogates. Chemosphere 111, 218-224.
551 Domino, M.M., Pepich, B.V., Munch, D.J., Fair, P.S. and Xie, Y. (2003) US EPA Method 552.3.
552 Determination of haloacetic acids and dalapon in drinking water by liquid-liquid microextraction,
553 derivatization, and gas chromatography with electron capture detection. EPA 815-B-03-002. US
554 EPA, Cincinnati, OH, USA.
555 Elovitz, M.S. and von Gunten, U. (1999) Hydroxyl radical/ozone ratios during ozonation processes. I.
556 the Rct concept. Ozone-Sci. Eng. 21(3), 239-260.
557 Elovitz, M.S., von Gunten, U. and Kaiser, H.-P. (2000) Hydroxyl radical/ozone ratios during
558 ozonation processes. II. the effect of temperature, pH, alkalinity, and DOM properties. Ozone-Sci.
559 Eng. 22(2), 123-150.
560 Escher, B.I., Dutt, M., Maylin, E., Tang, J.Y.M., Toze, S., Wolf, C.R. and Lang, M. (2012) Water
561 quality assessment using the AREc32 reporter gene assay indicative of the oxidative stress
562 response pathway. J. Environ. Monit. 14(11), 2877-2885.
563 Farré, M.J., Day, S., Neale, P.A., Stalter, D., Tang, J.Y. and Escher, B.I. (2013) Bioanalytical and
564 chemical assessment of the disinfection by-product formation potential: role of organic matter.
565 Water Res. 47(14), 5409-5421.
566 Gillogly, T., Najm, I., Minear, R., Marinas, B., Urban, M., Kim, J.H., Echigo, S., Amy, G., Douville,
567 C., Daw, B., Andrews, R., Hofmann, R. and Croué, J.-P. (2001) Bromate formation and control
568 during ozonation of low bromide waters, AWWA Research Foundation, Denver, CO, USA.

569 Glezer, V., Harris, B., Tal, N., Iosefvon, B. and Lev, O. (1999) Hydrolysis of haloacetonitriles: Linear
570 free energy relationship, kinetics and products. Water Res. 33(8), 1938-1948.
571 Hua, G. and Reckhow, D. (2007) Characterization of disinfection byproduct precursors based on
572 hydrophobicity and molecular size. Environ. Sci. Technol. 41, 3309-3315.
573 Hua, G. and Reckhow, D.A. (2013) Effect of pre-ozonation on the formation and speciation of DBPs.
574 Water Res. 47(13), 4322-4330.
575 Huang, H., Wu, Q.Y., Hu, H.Y. and Mitch, W.A. (2012) Dichloroacetonitrile and dichloroacetamide
576 can form independently during chlorination and chloramination of drinking waters, model organic
577 matters, and wastewater effluents. Environ. Sci. Technol. 46(19), 10624-10631.
578 Kleiser, G. and Frimmel, F.H. (2000) Removal of precursors for disinfection by-products (DBPs) -
579 differences between ozone- and OH-radical-induced oxidation. Sci. Total Environ. 256, 1-9.
580 Krasner, S.W. (2009) The formation and control of emerging disinfection by-products of health
581 concern. Philos. Trans. A Math. Phys. Eng. Sci. 367(1904), 4077-4095.
582 Le Lacheur, R.M. and Glaze, W.H. (1996) Reactions of ozone and hydroxyl radicals with serine.
583 Environ. Sci. Technol. 30, 1072-1080.
584 Lee, Y., Gerrity, D., Lee, M., Bogeat, A.E., Salhi, E., Gamage, S., Trenholm, R.A., Wert, E.C.,
585 Snyder, S.A. and von Gunten, U. (2013) Prediction of micropollutant elimination during ozonation
586 of municipal wastewater effluents: use of kinetic and water specific information. Environ. Sci.
587 Technol. 47(11), 5872-5881.
588 Lee, Y. and von Gunten, U. (2010) Oxidative transformation of micropollutants during municipal
589 wastewater treatment: comparison of kinetic aspects of selective (chlorine, chlorine dioxide, ferrate
590 VI, and ozone) and non-selective oxidants (hydroxyl radical). Water Res. 44(2), 555-566.
591 Lyon, B.A., Farre, M.J., De Vera, G.A., Keller, J., Roux, A., Weinberg, H.S. and Gernjak, W. (2013)
592 Organic matter removal and disinfection byproduct management in South East Queensland's
593 drinking water. Water Sci. Technol. Water Supply 14(4), 681-689.

Lyon, B.A., Milsk, R.Y., DeAngelo, A.B., Simmons, J.E., Moyer, M.P. and Weinberg, H.S. (2014) Integrated chemical and toxicological investigation of UV-chlorine/chloramine drinking water treatment. Environ. Sci. Technol. 48(12), 6743-6753.

Magdeburg, A., Stalter, D., Schlusener, M., Ternes, T. and Oehlmann, J. (2014) Evaluating the efficiency of advanced wastewater treatment: target analysis of organic contaminants and (geno-) toxicity assessment tell a different story. Water Res. 50, 35-47.

Molnar, J.J., Agbaba, J.R., Dalmacija, B.D., Klasnja, M.T., Dalmacija, M.B. and Kragulj, M.M. (2012a) A comparative study of the effects of ozonation and TiO_2-catalyzed ozonation on the selected chlorine disinfection by-product precursor content and structure. Sci. Total Environ. 425, 169-175.

Molnar, J., Agbaba, J., Dalmacija, B., Roncevic, S., Prica, M. and Tubic, A. (2012b) Influence of pH and ozone dose on the content and structure of haloacetic acid precursors in groundwater. Environ. Sci. Pollut. Res. Int. 19(8), 3079-3086.

Neale, P.A., Antony, A., Bartkow, M.E., Farre, M.J., Heitz, A., Kristiana, I., Tang, J.Y. and Escher, B.I. (2012) Bioanalytical assessment of the formation of disinfection byproducts in a drinking water treatment plant. Environ. Sci. Technol. 46(18), 10317-10325.

Nöthe, T., Fahlenkamp, H. and Von Sonntag, C. (2009) Ozonation of wastewater: rate of ozone consumption and hydroxyl radical yield. Environ. Sci. Technol. 43, 5590-5595.

Petala, M., Samaras, P., Zouboulis, A., Kungolos, A. and Sakellaropoulos, G.P. (2008) Influence of ozonation on the in vitro mutagenic and toxic potential of secondary effluents. Water Res. 42(20), 4929-4940.

Plewa, M.J., Wagner, E.D., Muellner, M.G., Hsu, K.-M. and Richardson, S.D. (2008) Comparative mammalian cell toxicity of N-DBPs and C-DBPs. Ch. 3 in Disinfection By-Products in Drinking Water. ACS Symposium Series, American Chemical Society, Washington, DC, USA.

Ratpukdi, T., Siripattanakul, S. and Khan, E. (2010) Mineralization and biodegradability enhancement of natural organic matter by ozone-VUV in comparison with ozone, VUV, ozone-UV, and UV: effects of pH and ozone dose. Water Res. 44(11), 3531-3543.

Reifferscheid, G., Heil, J., Oda, Y. and Zahn, R.K. (1991) A microplate version of the SOS/*umu*-test for rapid detection of genotoxins and genotoxic potentials of environmental samples. Mutat. Res. 253(3), 215-222.

Reisz, E., Fischbacher, A., Naumov, S., von Sonntag, C. and Schmidt, T.C. (2014) Hydride transfer: a dominating reaction of ozone with tertiary butanol and formate ion in aqueous solution. Ozone-Sci. Eng. 36(6), 532-539.

Reungoat, J., Macova, M., Escher, B.I., Carswell, S., Mueller, J.F. and Keller, J. (2010) Removal of micropollutants and reduction of biological activity in a full scale reclamation plant using ozonation and activated carbon filtration. Water Res. 44(2), 625-637.

Shah, A.D. and Mitch, W.A. (2012) Halonitroalkanes, halonitriles, haloamides, and N-nitrosamines: a critical review of nitrogenous disinfection byproduct formation pathways. Environ. Sci. Technol. 46(1), 119-131.

Shan, J., Hu, J., Kaplan-Bekaroglu, S.S., Song, H. and Karanfil, T. (2012) The effects of pH, bromide and nitrite on halonitromethane and trihalomethane formation from amino acids and amino sugars. Chemosphere 86(4), 323-328.

Singer, P.C., Harrington, G.W., Cowman, G.A., Smith, M.E., Schechther, D.S. and Harrington, L.J. (1999) Impacts of ozonation on the formation of chlorination and chloramination by-products, AWWA Research Foundation, Denver, CO, USA.

Stalter, D., Magdeburg, A. and Oehlmann, J. (2010) Comparative toxicity assessment of ozone and activated carbon treated sewage effluents using an in vivo test battery. Water Res. 44(8), 2610-2620.

642 Tang, J.Y.M., McCarty, S., Glenn, E., Neale, P.A., Warne, M.S.J. and Escher, B.I. (2013) Mixture
643 effects of organic micropollutants present in water: Towards the development of effect-based water
644 quality trigger values for baseline toxicity. Water Res. 47(10), 3300-3314.
645 von Gunten, U. (2003a) Ozonation of drinking water: Part II. Disinfection and by-product formation
646 in presence of bromide, iodide or chlorine. Water Res. 37, 1469-1487.
647 von Gunten, U. (2003b) Ozonation of drinking water: Part I. Oxidation kinetics and product
648 formation. Water Res. 37(7), 1443-1467.
649 von Gunten, U. and Hoigné, J. (1994) Bromate formation during ozonation of bromide-containing
650 waters: interaction of ozone and hydroxyl radical reaction. Environ. Sci. Technol. 28(7), 1234-
651 1242.
652 von Gunten, U. and Oliveras, Y. (1998) Advanced oxidation of bromide-containing waters; bromate
653 formation mechanism. Environ. Sci. Technol. 32, 63-70.
654 von Sonntag, C. (2008) Advanced oxidation processes: mechanistic aspects. Water Sci. Technol.
655 58(5), 1015-1021.
656 Wenk, J., Aeschbacher, M., Salhi, E., Canonica, S., von Gunten, U. and Sander, M. (2013) Chemical
657 oxidation of dissolved organic matter by chlorine dioxide, chlorine, and ozone: effects on its
658 optical and antioxidant properties. Environ. Sci. Technol. 47(19), 11147-11156.
659 Westerhoff, P., Aiken, G., Amy, G. and Derboux, J. (1999) Relationships between the structure of
660 natural organic matter and its reactivity towards molecular ozone and hydroxyl radicals. Water Res.
661 33(10), 2265-2276.
662 Westerhoff, P., Chao, P. and Mash, H. (2004) Reactivity of natural organic matter with aqueous
663 chlorine and bromine. Water Res. 38(6), 1502-1513.
664 Xie, Y., Rashid, I., Zhou, H. and Gammie, L. (2002) Acidic methanol methylation for HAA analysis:
665 limitations and possible solutions. J. Am. Water Works Ass. 94(11), 115-122.

Yang, X., Peng, J., Chen, B., Guo, W., Liang, Y., Liu, W. and Liu, L. (2012a) Effects of ozone and ozone/peroxide pretreatments on disinfection byproduct formation during subsequent chlorination and chloramination. J. Hazard. Mater. 239-240, 348-354.

Yang, X., Shang, C., Shen, Q., Chen, B., Westerhoff, P., Peng, J. and Guo, W. (2012b) Nitrogen origins and the role of ozonation in the formation of haloacetonitriles and halonitromethanes in chlorine water treatment. Environ. Sci. Technol. 46(23), 12832-12838.

Yeh, R.Y., Farré, M.J., Stalter, D., Tang, J.Y., Molendijk, J. and Escher, B.I. (2014) Bioanalytical and chemical evaluation of disinfection by-products in swimming pool water. Water Res. 59, 172-184.

Zhang, P. and Jian, L. (2006) Ozone-enhanced photocatalytic degradation of natural organic matter in water. Water Sci. Technol. Water Supply 6(3), 53-61.

Figure Captions:

Figure 1. Formation potentials (FP) of (a) C-DBPs and (b) N-DBPs in the presence and absence of t-BuOH and H_2O_2. Conditions: TOC = 17.2 ± 2.0 mg/L, transferred ozone dose = 0.75 mg/mg TOC, pH = 7 (1 mM phosphate), t-BuOH = 10 mM, H_2O_2 = 1 mg/mg O_3, temperature = 22±1 ^{0}C. HOCl DBP 24 h formation potentials tests at pH 7 were targeted to have a 1 – 2 mg/L Cl_2 residual. Error bars depict standard deviation of 3 replicate experiments.

Figure 2. Formation potentials of (a) C-DBPs and (b) N-DBPs at different ozonation pH. Conditions: TOC = 17.2 ± 2.0 mg/L, transferred ozone dose = 0.75 mg/mg TOC, buffer = 1 mM phosphate, temperature = 22 ± 1 ^{0}C. HOCl DBP 24 h formation potentials tests at pH 7 were targeted to have a 1 – 2 mg/L Cl_2 residual. Error bars depict standard deviation of 3 replicate experiments.

Figure 3. Formation potentials of (a) C-DBPs and (b) N-DBPs at different transferred ozone doses. Conditions: TOC = 17.2 ± 2.0 mg/L, pH =7 (1 mM phosphate), temperature = 22 ± 1°C. HOCl DBP 24 h formation potentials tests at pH 7 were targeted to have a 1 – 2 mg/L Cl_2 residual. Error bars depict standard deviation of 3 replicate experiments.

Figure 4. Changes in (a) AOX and (b) unknown/known AOX after ozonation and subsequent chlorination (n=2). TOC = 16.4 ± 2.0 mg/L; first set of bars in each plot correspond to samples ozonated with and without t-BuOH and H_2O_2; the second set were treated at different ozonation pH values (buffered with 1 mM phosphate); the third set were ozonated with increasing ozone dose (0.4 – 1 mg/mg TOC). Error bars depict the absolute difference.

Figure 5. Relationship of AOX formation potentials to bioassay results (Microtox, umuC, AREc32, p53) of samples ozonated at different conditions prior to chlorination (n=2). Bioassay results show the range of effect concentrations (EC_{50} and $EC_{IR1.5}$) in units of relative enrichment factor (REF).

Numbered symbols (E) correspond to the results of 6 experiments, namely ozonation at different O_3 doses (0, 0.4, 0.75 (also for pH 7), 1 mg O_3/mg TOC) and pH (6, 8). Circle and inverted triangle symbols correspond to samples treated with O_3/t-BuOH and O_3/H_2O_2, respectively. Error bars depict the absolute difference.

Figure 1:

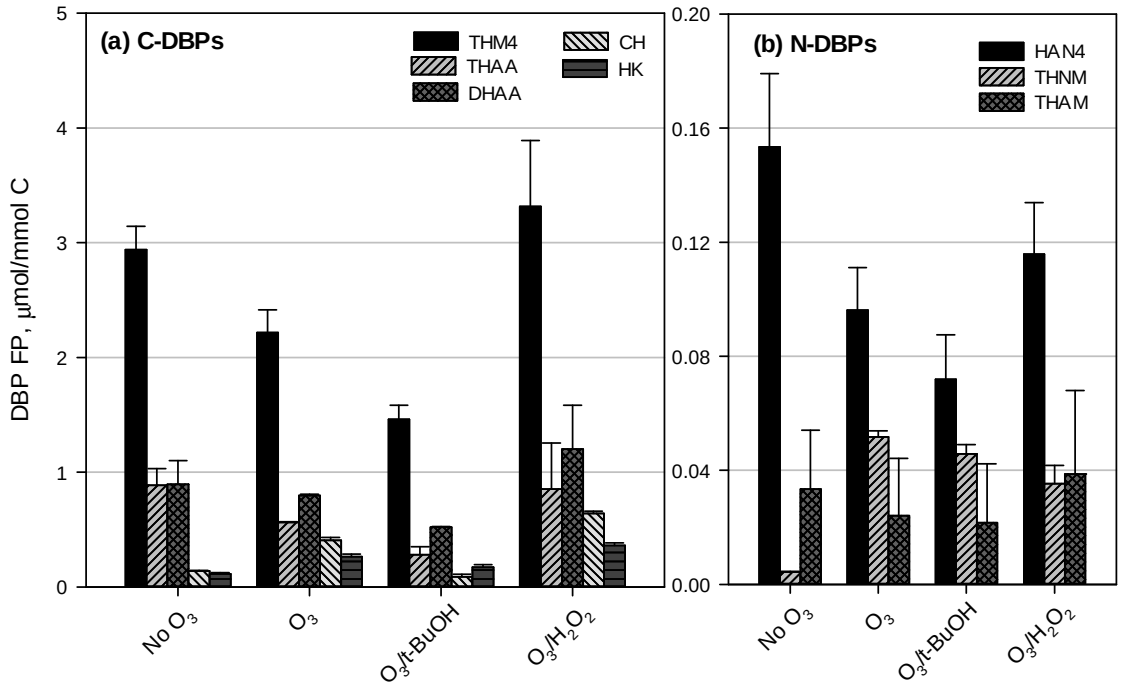

Figure 2:

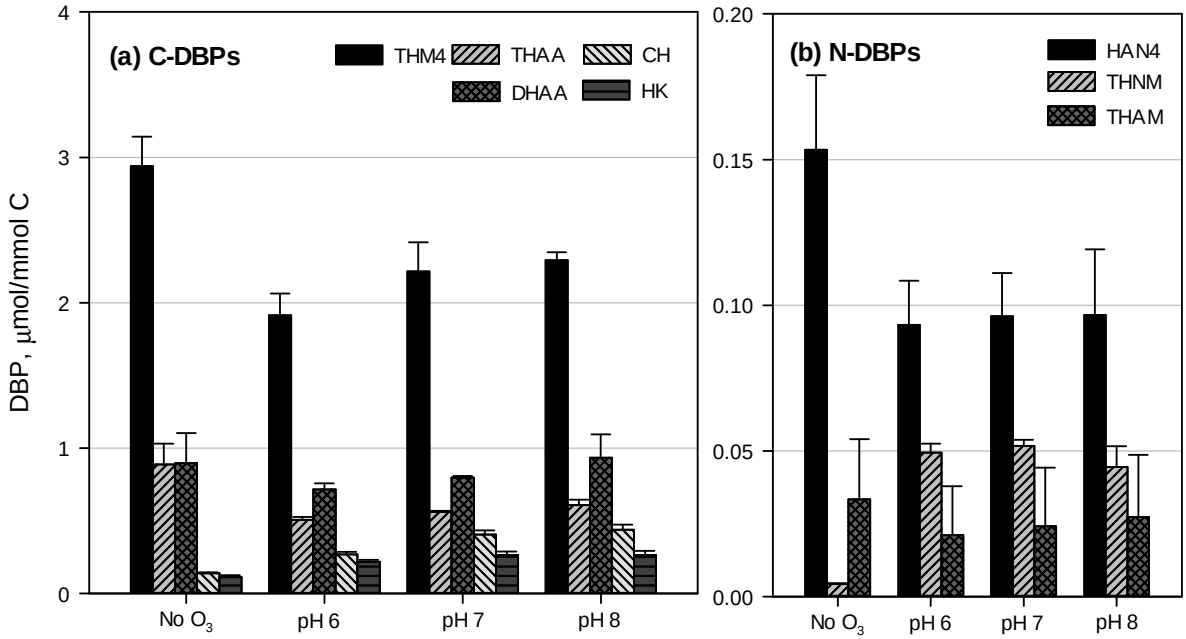

Figure 3:

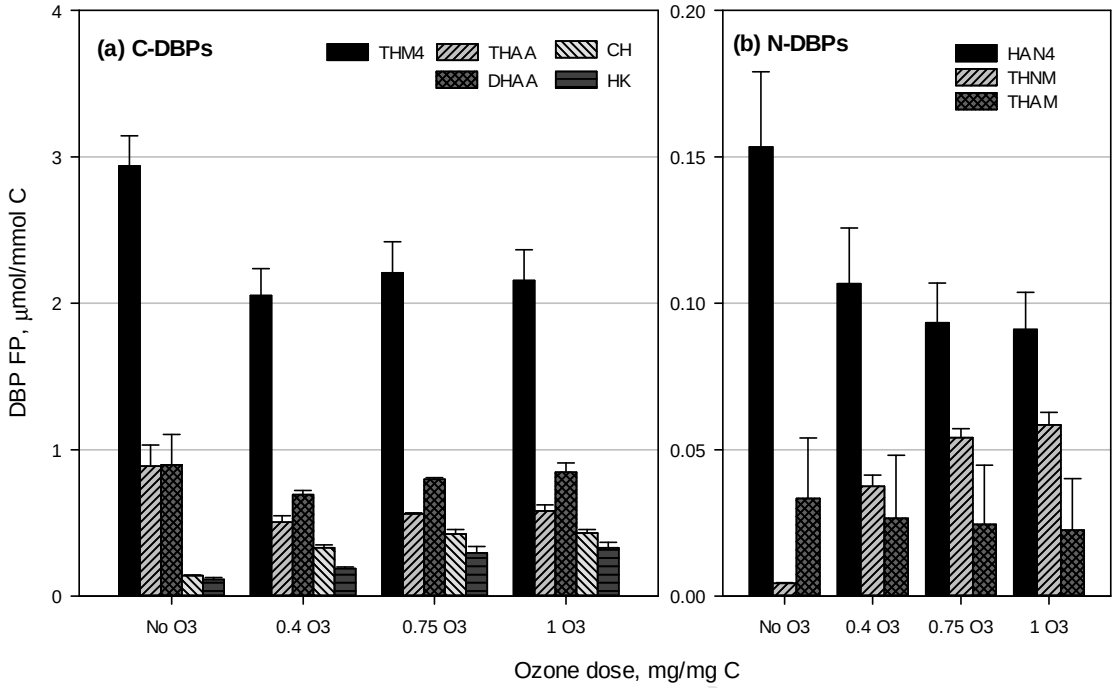

Figure 4:

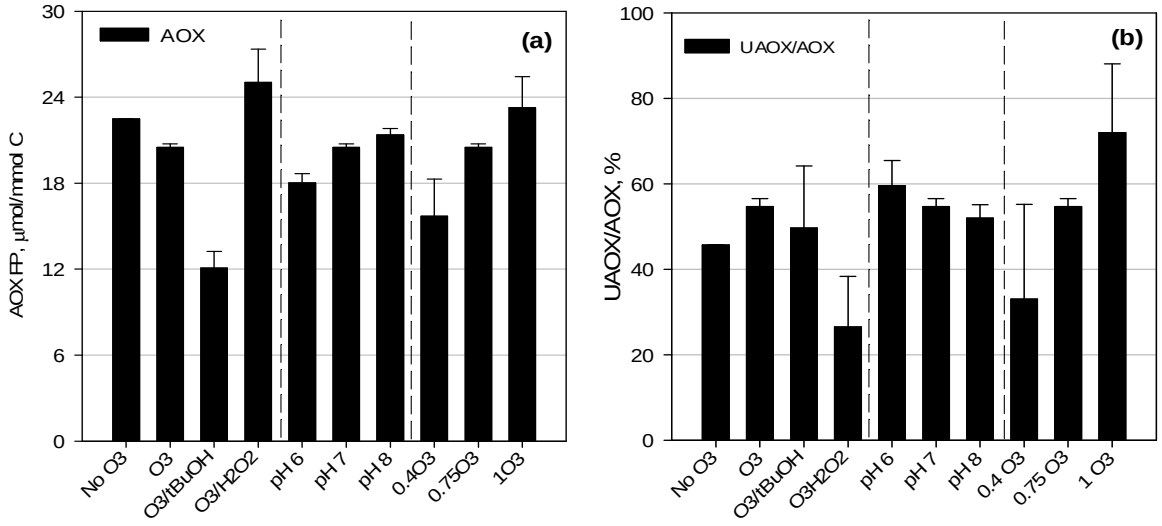

Figure 5:

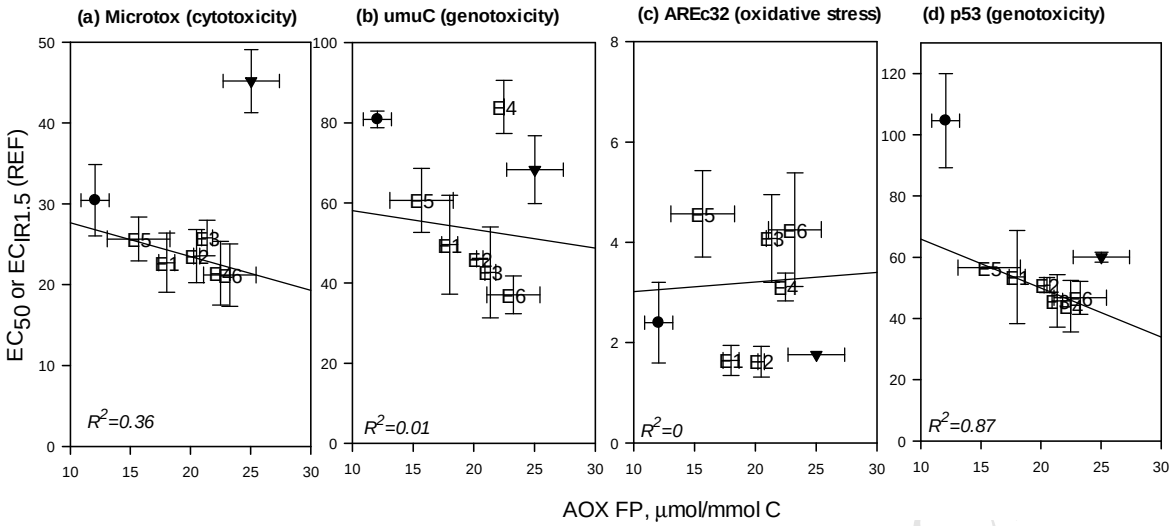

Highlights

- O_3/˙OH ratios were modified to investigate DBP formation in drinking water
- Compared to ˙OH, oxidation by O_3 led to less C-DBPs and AOX formation potential
- HAN4 and THAMs showed opposite trends to THNM formation when modifying O_3/˙OH ratio
- 4 bioassays showed low differences in toxicity between different O_3/˙OH exposures

Appendix A. Supplementary Data for

Towards reducing DBP formation potential of drinking water by favouring direct ozone over hydroxyl radical reactions during ozonation

Glen Andrew De Vera[*], Daniel Stalter[‡,‖], Wolfgang Gernjak[*,§], Howard S. Weinberg[#], Jurg Keller[*], Maria José Farré[*,§,†]

[*]The University of Queensland, Advanced Water Management Centre, Queensland 4072, Australia

[‡]The University of Queensland, National Research Centre for Environmental Toxicology (Entox), Brisbane, Queensland 4108, Australia

[§]ICRA, Catalan Institute for Water Research, Scientific and Technological Park of the University of Girona, H_2O Building, Emili Grahit 101, 17003 Girona, Spain

[#]University of North Carolina at Chapel Hill, Department of Environmental Sciences and Engineering, 146A Rosenau Hall, Chapel Hill, North Carolina 27599, United States

[‖]Swiss Federal Institute of Aquatic Science and Technology (EAWAG), Überlandstrasse 133, Dübendorf 8600, Switzerland.

[†]Corresponding author: Maria José Farré: phone: (+34) 972 18 33 80, email: mjfarre@icra.cat

Submitted to Water Research

This file includes:

4 texts, 4 tables, and 11 figures addressing experimental procedure and additional data

Text S1. Reverse osmosis system for sample concentration

The reverse osmosis (RO) system (Biopure 962, QLD, Australia) included two polyamide spiral wound membranes (RE-2521BE, Biopure, QLD, Australia), three polyspun sediment filters (0.5, 1, 5 μm) (Hydrotwist, Australia) and two cation exchange resin cartridges containing Tulsion T-42 strong cation exchange resin in Na^+ and H^+ form (Thermax, India). Prior to use of the system, cation exchange resins were rinsed with deionized water for about one week until no impurities were detected in the filtered water by absorbance and fluorescence measurements. The 1000 L settled water was first passed through the sediment filters once and collected in 200 L reservoirs. The RO system was operated until 20 L of concentrate was collected. The concentrate was then stored in high density polyethylene bottles (QHFSS, QLD, Australia) and frozen until use. Characteristics of the original water sample and RO concentrate are shown in Table S1. Because of the decrease in pH with use of cation exchange resins in H^+-form, no inorganic carbon was detected in the concentrate. It can also be noted that concentration factors of dissolved organic carbon and nitrogen are 37 and 20, respectively. The lower concentration factor for organic nitrogen is possibly due to loss of low molecular-size organics during NOM isolation (Gjessing et al. 1999, Sun et al. 1995). The lost organic nitrogen fractions could also be precursors of HANs as observed in the lower DBP formation potential compared to the actual sample (Table S2).

Text S2. Preparation of ozone stock solution

Ozone stock solutions (1 − 1.5 mM O_3) were prepared by sparging gaseous ozone through 500 mL of deionized water (obtained from a MilliQ Advantage system, Millipore, Australia) that was cooled in an ice bath to a temperature near 0°C. Gaseous ozone was generated from pure oxygen (99.995%; Coregas, QLD, Australia) using an Anseros COM-AD-04 ozone generator (Tübingen, Germany). The stock solutions were standardized spectrophotometrically using the absorbance at 258 nm (ε=3000 $M^{-1}cm^{-1}$) (Elovitz and von Gunten 1999) measured with a Varian Cary 50 Bio UV-Visible spectrophotometer (Mulgrave, VIC, Australia). Appropriate volumes of the ozone stock solution were spiked into samples to reach the desired ozone concentration.

Text S3. Characterization of ozonated samples

Total organic carbon (TOC): The TOC was measured with a Shimadzu TOC-L total organic carbon analyser with a TNM-L total nitrogen analyzer unit and ASI-L autosampler (Shimadzu, Kyoto, Japan).

UV-Visible absorbance: UV-visible absorbance was measured from 600-200 nm in a quartz cuvette with a Varian Cary 50 Bio UV-Visible spectrophotometer. $SUVA_{254}$ was calculated by multiplying the UV absorbance at 254 nm (cm^{-1}) by 100 and then dividing by the TOC (mg-C/L) to obtain units of L/mg-C·m.

Excitation Emission Matrix (EEM) fluorescence: Fluorescence measurements were performed in a quartz cuvette using a PerkinElmer LS-55 luminescence spectrometer (Perkin Elmer, Australia). EEM measurements were made from 200 – 400 nm excitation wavelengths and 280 – 500 nm emission wavelengths. Regional integration of the fluorescence spectra using R statistical software (R Foundation for Statistical Computing, Vienna, Austria) was used to classify components of NOM according to the regions of Chen et al. (2003).

Aldehyde analysis: Formaldehyde, acetaldehyde, glyoxal and methyl glyoxal were extracted within 1 week after ozonation of the sample. These aldehydes were extracted using EPA Method 556 (Munch et al. 1998). The following standards were used: formaldehyde (36.5 – 38% in water, Sigma-Aldrich, St. Louis, MO, USA), acetaldehyde (≥99.5%, Sigma-Aldrich, Switzerland), glyoxal (40% in water, Sigma-Aldrich, Germany), methylglyoxal (40% in water, Sigma, Germany), 4-fluorobenzaldehyde (surrogate standard, 98%, Aldrich, Hong Kong), and 1,2-dibromopropane (internal standard, 97%, Aldrich, USA). In this method, the analytes were derivatized in aqueous solution to their corresponding pentafluorobenzyl oximes using *O*-(2,3,4,5,6-pentafluorobenzyl hydroxylamine hydrochloride (≥99.0%, Fluka, Switzerland) and were extracted using hexane (B&J GC^2, Honeywell, Muskegon, MI, USA). The extracts were analyzed by GC/ECD. The reporting limit for the 4 aldehydes was 0.2 µg/L with recoveries ranging from 80 – 120%.

Inorganic nitrogen: Ammonia, nitrite and total NO_x were measured on a Lachat QuikChem8500 Flow Injection Analyzer (Hach Company, CO, USA) using Lachat QuickChem method 31-107-06-1-A. The detection limit for both ions is 2.0 µg/L.

Text S4. DBP standards

The following DBP standards were purchased from the following suppliers: THM4 calibration mix (TCM, DBCM, BDCM, and TBM; 2000 µg/mL each in methanol, Supelco, Bellefonte, PA, USA), EPA 551B halogenated volatiles mix (BCAN, DBAN, DCAN, 1,1-DCP, 1,1,1-TCP, TCAN, and TCNM; 2000 µg/mL each in acetone, Supelco, Bellefonte, PA, USA), CH (>99.5%, Sigma-Aldrich 15307, Belgium), and TCAM (99%, Aldrich 217344, Switzerland). The standards for TBNM and

other THAMs were purchased with >99% purity from Orchid Cellmark, Canada. 1,2-dibromopropane (97%, Aldrich, USA) was used as the internal standard.

Table S1. Settled water and RO concentrate characteristics

Parameter (units)	Original settled water sample (feed)	RO concentrate
TOC (mg C/L)	4.8±0.1	181±3
TON (mg N/L)	0.3	6.0
SUVA 254 (L/mg-C·m)	1.7	1.9±0.1
Inorganic carbon (mg C/L)	2.5±0.1	<0.5
Bromide (mg/L)	0.1	3.2±0.1
Iodide (mg/L)	<0.1	<0.1

Table S2. Comparison of volatile DBP formation potentials (μmol/mmol C×10^2) of original settled water (4.8 mg/L TOC) and reconstituted water samples (19.5 mg/L TOC)

DBPs	Original settled water sample	Reconstituted sample
Trihalomethanes (THM4)	295	280
Trichloromethane (TCM)	206	201
Bromodichloromethane (BDCM)	74	68
Dibromochloromethane (DBCM)	15	11
Tribromomethane (TBM)	0.8	0.4
Haloacetonitriles (HAN4)	30	17
Trichloroacetonitrile (TCAN)	0.8	0.3
Dichloroacetonitrile (DCAN)	23	13
Bromochloroacetonitrile (BCAN)	5.0	3.7
Dibromoacetonitrile (DBAN)	1.0	0.5
Chloral hydrate (CH)	16	16
Halonitromethanes (THNM)	1.4	0.7
Trichloronitromethane (TCNM)	0.9	0.5
Tribromonitromethane (TBNM)	<0.02	0.2
Haloketones (HK)	16	11
1,1-dichloropropanone (11DCP)	1.0	0.8
1,1,1,-trichloropropanone (111TCP)	15	11
Trihaloacetamides (THAM)	6.6	7.1
Trichloroacetamide (TCAM)	3.5	3.6
Bromodichloroacetamide (BDCAM)	3.1	2.0
Dibromochloroacetamide (DBCAM)	< 0.1	1.5

Table S3. Average formation potentials of DBPs (μmol/mmolC×10^2) during ozonation at different conditions*. Numbers in parentheses are the standard deviation (n=3) and absolute difference (n=2).[a]

DBP	No O_3	O_3/pH 7/0.75 O_3	O_3/t-BuOH	O_3/H_2O_2	pH 6	pH 8	0.4 O_3	1 O_3
Trichloromethane (TCM)	225 (13)	156 (23)	77 (8)	256 (56)	128 (19)	163(6)	140 (21)	152 (24)
Bromodichloromethane (BDCM)	59 (8)	52 (3)	54 (3)	63 (3)	49 (2)	52 (6)	50 (3)	51 (2)
Dibromochloromethane (DBCM)	9.0 (2.3)	12 (3)	14 (1)	12 (2)	13 (2)	13 (2)	14 (3)	12 (2)
Tribromomethane (TBM)	0.3 (0.1)	1.0 (0.4)	1.6 (1.0)	0.7 (0.2)	1.0 (0.4)	1.0 (0.3)	1.3 (0.5)	0.9 (0.4)
Monochloroacetic acid (MCAA)[a]	9.2 (6.7)	<3.7	17 (3)	19 (2)	13 (4)	15 (6)	11 (4)	16 (6)
Monobromoacetic acid (MBAA)[a]	<2.5	3.3 (0.8)	4.6 (0.1)	<2.5	5.6 (0.3)	<2.5	<2.5	5.1 (0.2)
Dichloroacetic acid (DCAA)[a]	70 (26)	60 (1)	34 (0)	101 (53)	52 (6)	73 (21)	51 (3)	64 (8)
Trichloroacetic acid (TCAA)[a]	66 (15)	36 (4.)	16 (4)	61 (41)	33 (6)	40 (3)	32 (8)	38 (9)
Bromochloroacetic acid (BCAA)[a]	17 (3)	16 (0.0)	11 (0)	16 (2)	14 (0)	17 (1)	15 (1)	15 (0)
Bromodichloroacetic acid (BDCAA)[a]	19 (4)	16 (1)	8.7 (4.4)	19 (10)	14 (1)	16 (4)	14 (0)	16 (0)
Dibromoacetic acid (DBAA)[a]	2.9 (0.6)	4.3 (0.1)	7.1 (0.4)	3.2 (0.1)	6.2 (0.2)	4.0 (0.7)	4.0 (0.0)	4.9 (0.2)
Chlorodibromoacetic acid (CDBAA)[a]	3.4 (1.7)	4.3 (2.3)	3.5 (2.0)	5.5 (6.0)	3.8 (1.9)	4.7 (3.7)	4.0 (1.6)	4.3 (2.3)
Trichloroacetonitrile (TCAN)	0.2 (0.1)	0.2 (0.0)	0.2 (0.2)	0.2 (0.1)	0.2 (0.0)	0.2 (0.1)	0.2 (0.0)	0.3 (0.0)
Dichloroacetonitrile (DCAN)	12 (2)	6.5 (0.9)	4.2 (1.1)	8.3 (1.2)	6.5 (1.0)	6.5 (1.7)	6.9 (1.0)	6.5 (0.8)
Bromochloroacetonitrile (BCAN)	3.1 (0.9)	2.1 (0.4)	1.8 (0.5)	2.6 (0.7)	2.0 (0.4)	2.3 (0.6)	2.8 (0.8)	1.9 (0.4)
Dibromoacetonitrile (DBAN)	0.4 (0.0)	0.6 (0.1)	0.9 (0.1)	0.6 (0.1)	0.7 (0.1)	0.7 (0.1)	0.8 (0.1)	0.6 (0.1)
Chloral hydrate (CH)	14 (1)	43 (3)	8.7 (2.4)	64 (2)	27 (2)	44 (4)	33 (2)	43 (3)
Trichloronitromethane (TCNM)	0.4 (0.1)	5.1 (0.3)	3.6 (0.2)	3.4 (0.6)	4.6 (0.4)	4.2 (0.6)	3.5 (0.3)	5.5 (0.5)
Tribromonitromethane (TBNM)	0.04 (0.07)	0.3 (0.1)	1.0 (0.2)	0.1 (0.1)	0.4 (0.1)	0.3 (0.1)	0.2 (0.1)	0.3 (0.1)
1,1-dichloropropanone (11DCP)	1.0 (0.6)	1.8 (1.4)	1.8 (0.3)	1.9 (0.5)	1.4 (0.7)	2.2 (1.0)	1.0 (0.4)	1.9 (1.4)
1,1,1,-trichloropropanone (111TCP)	10 (1)	28 (3)	16 (2)	35 (2)	20 (2)	24 (3)	18 (1)	31 (4)
Trichloroacetamide (TCAM)	2.1 (1.0)	1.2 (0.8)	0.5 (0.3)	1.8 (1.0)	0.9 (0.5)	1.3 (0.8)	1.1 (0.6)	1.0 (0.6)
Bromodichloroacetamide (BDCAM)[a]	1.1 (0.1)	0.9 (0.3)	0.9 (0.0)	1.8 (0.8)	0.8 (0.3)	1.0 (0.4)	1.0 (0.2)	0.9 (0.4)
Dibromochloroacetamide (DBCAM)[a]	0.5 (0.2)	1.0 (0.8)	1.6 (1.9)	1.3 (0.7)	1.0 (0.9)	1.1 (0.6)	1.4 (1.2)	1.1 (0.6)
Adsorbable organic halogen (AOX)[a]	2250 (1)	2050 (50)	1210 (234)	2500 (467)	1800 (133)	2140 (89)	1570 (522)	2330 (436)

[*] *average values from experiments (n=3; n=2 for HAAs, BDCAM, DBCAM, and AOX) with two extractions per sample and TOC = 17±2mg/L; Chlorine residuals normally ranged from 1 to 2 mg Cl_2/L.*

Table S4. Average percent removal of DBP formation potentials under ozone- and OH-dominant conditions*

DBP	O_3 pathway		Control (ozonated, pH 7, no t-BuOH and H_2O_2)	$^{\bullet}OH$ pathway	
	pH 6	O_3/t-BuOH		pH 8	O_3/H_2O_2
THM4	35	50	25	22	-13
HAN4	39	53	37	37	25
CH	-94	37	-192	-215	-361
THNM	-1028	-945	-1079	-915	-706
HK	-91	-51	-133	-131	-219
THAM	37	35	28	18	-16
THAA	43	68	37	32	4
DHAA	20	42	11	-4	-34
AOX	20	46	9	5	-11

**calculated from DBP formation potentials of non-ozonated water sample*

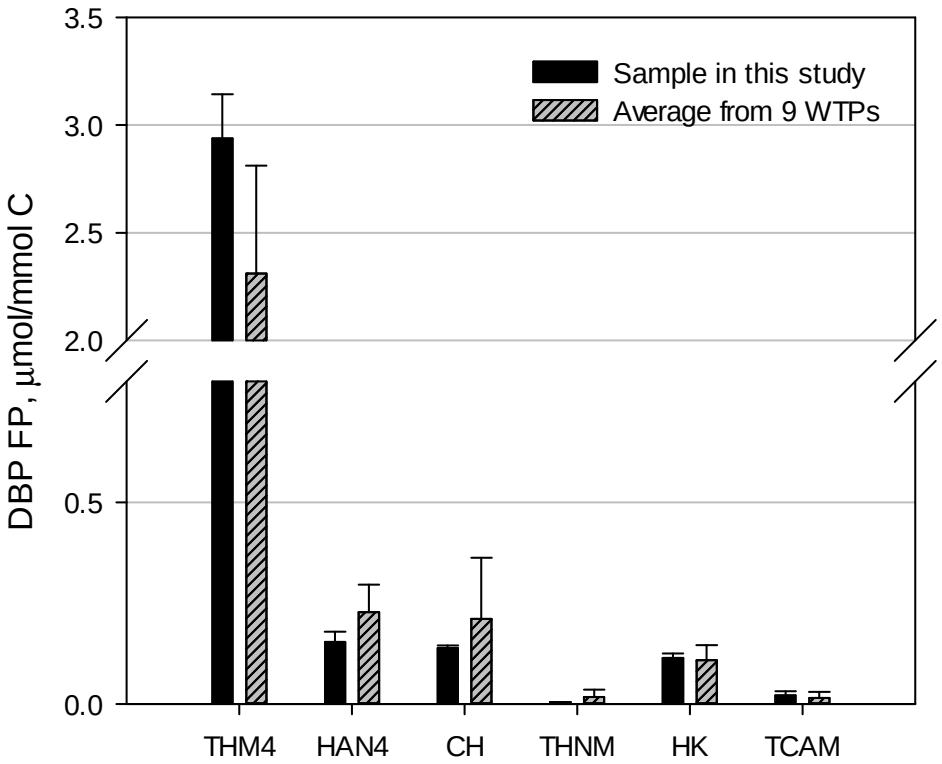

Figure S1. Comparison between DBP formation potentials of settled water sample used in this study and of samples taken from 9 different drinking water treatment plants (WTPs) in South East Queensland, Australia.

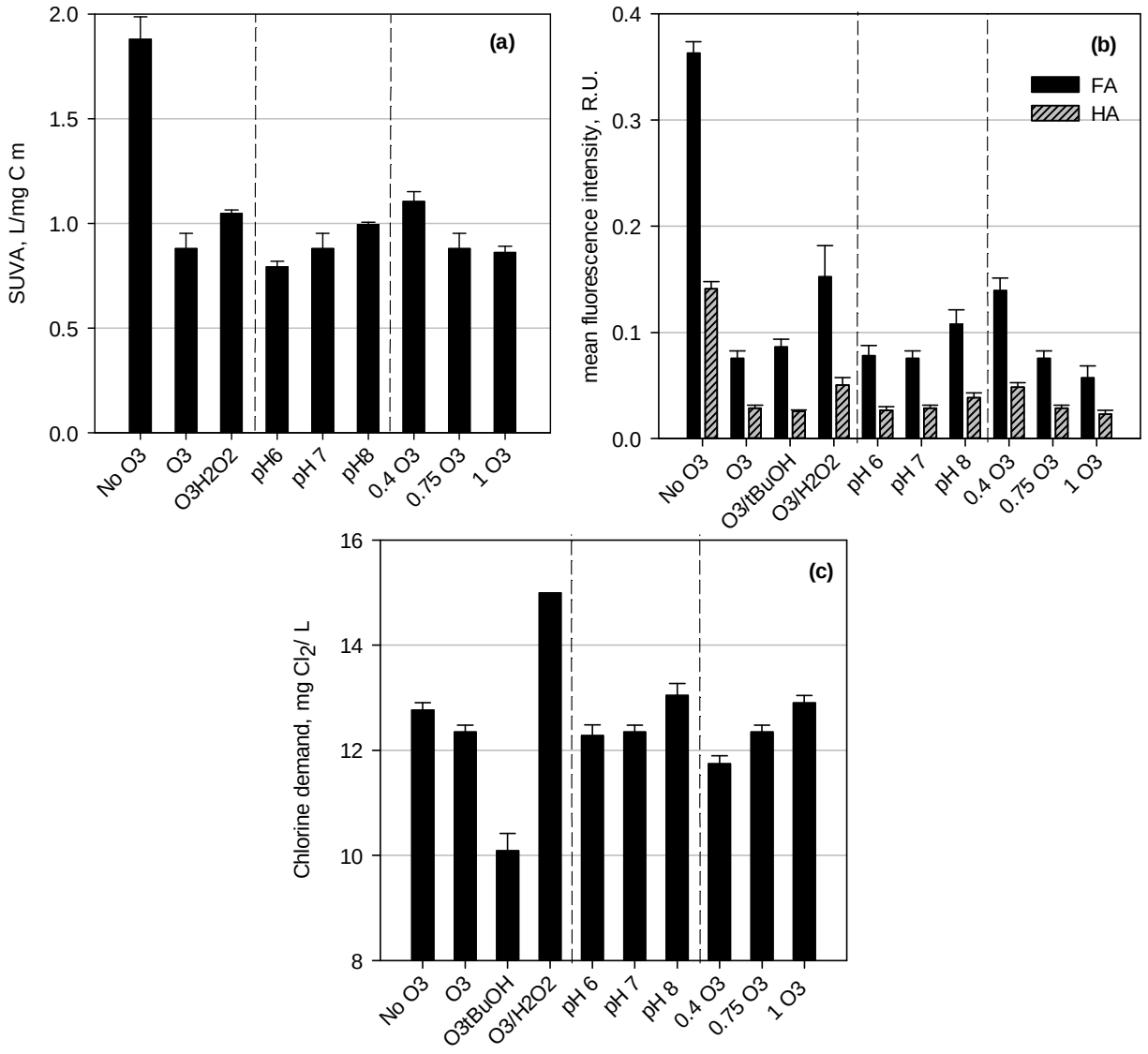

Figure S2. Changes in (a) SUVA, (b) fluorescence of fulvic acid- (FA) and humic acid (HA)-like EEM regions, and (c) chlorine demand of samples after ozonation for different oxidant exposures. Error bars depict the standard deviation of 3 replicate experimental results. Reported fluorescence measurements (R.U. = Raman Units) were taken from samples diluted 4-fold.

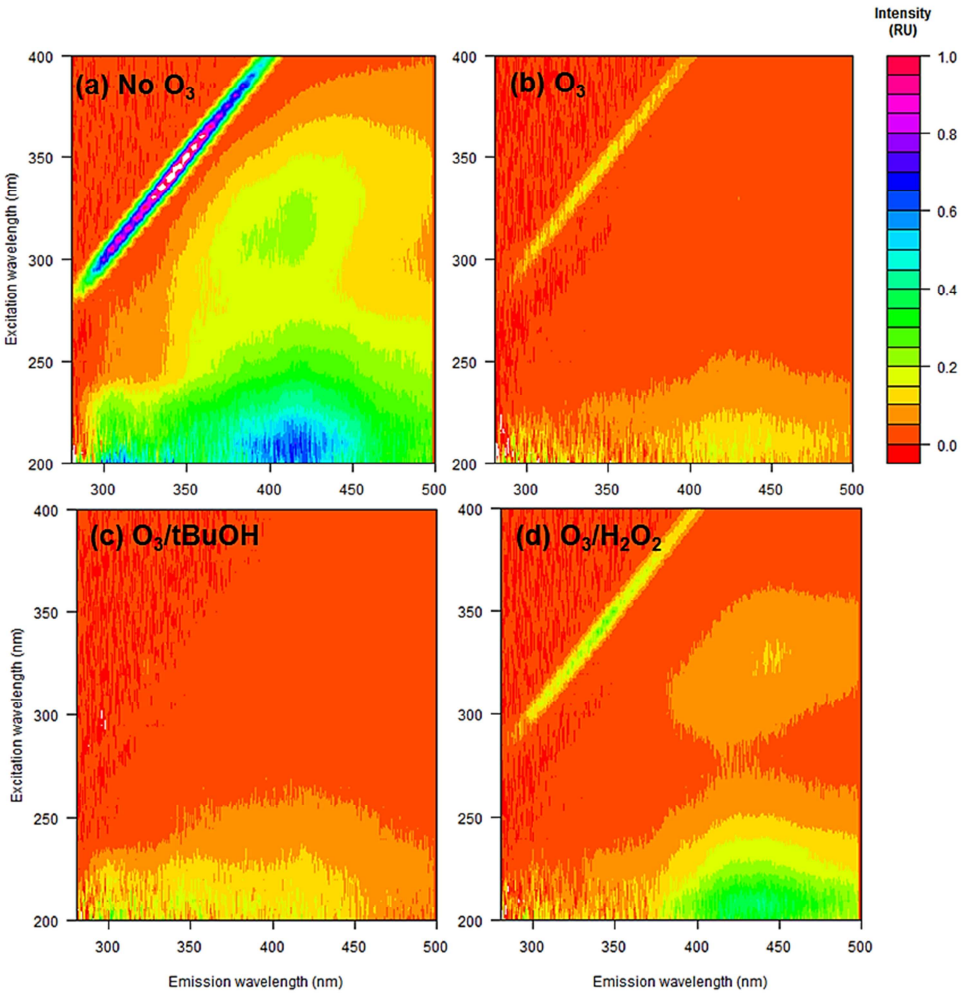

Figure S3. Example fluorescence EEM plots showing the influence of O_3 and $^{\bullet}OH$ on NOM characteristics.

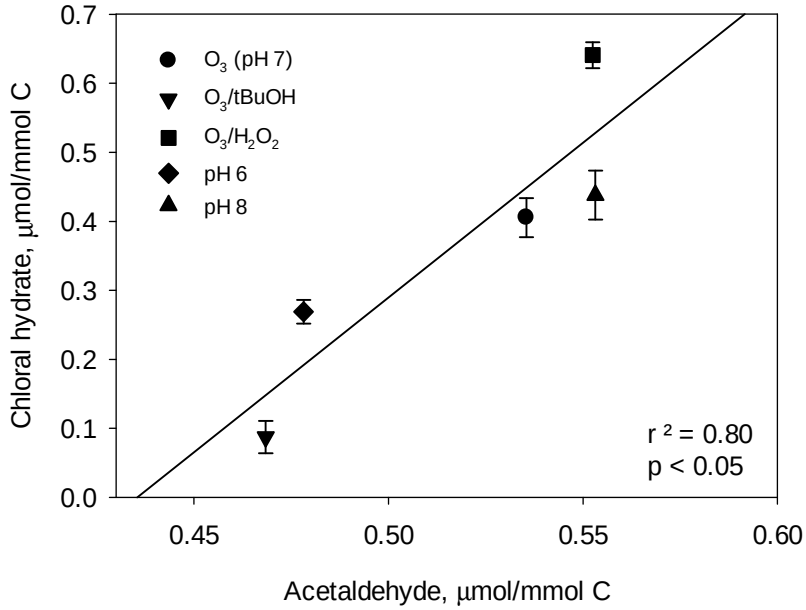

111

112 Figure S4. Correlation between acetaldehyde formation after ozonation and chloral hydrate
113 formation after subsequent chlorination of the same sample. Conditions: TOC = 18 mg/L; transferred
114 ozone dose = 0.75 mg O_3/mg TOC.

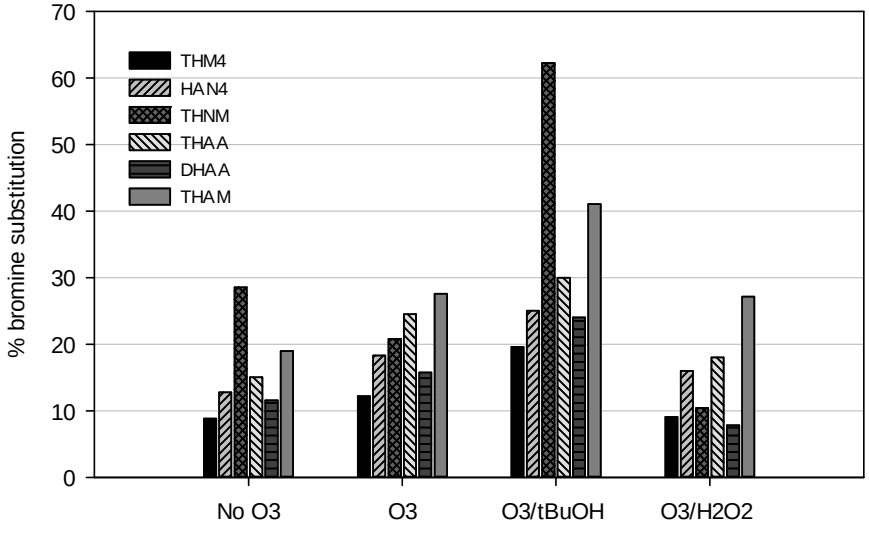

115

116 Figure S5. Effect of molecular ozone and •OH pathways on percent bromine substitution of C- and
117 N-DBPs following subsequent chlorination.

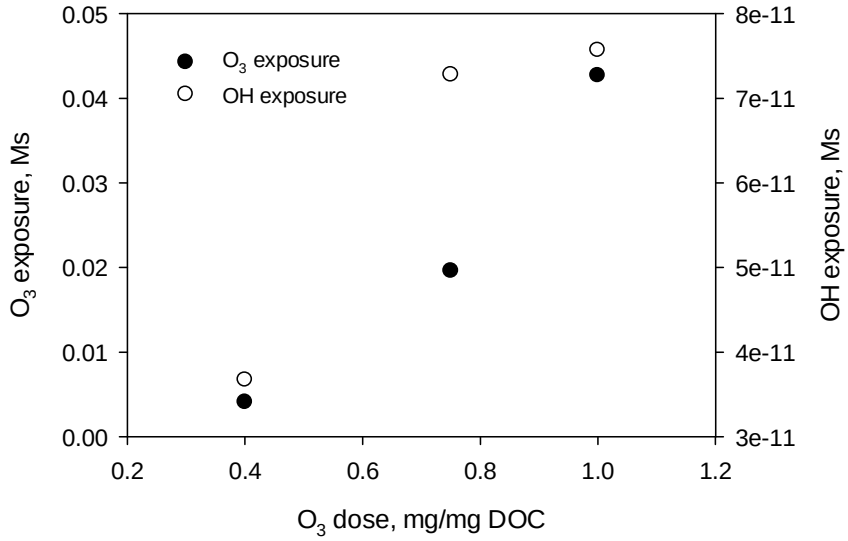

118

119 Figure S6. Increase in O_3 and $^{\bullet}OH$ exposures during ozonation of reconstituted RO concentrate with
120 increase in transferred ozone dose. Conditions: TOC = 20 mg/L, TON = 0.7 mg/L, pH = 7,
121 temperature = 22 ± 1°C; Ozone exposures were measured using the indigo method while $^{\bullet}OH$
122 exposures were indirectly determined through decay of *para*-chlorobenzoic acid (1 μM) (Elovitz and
123 von Gunten 1999).

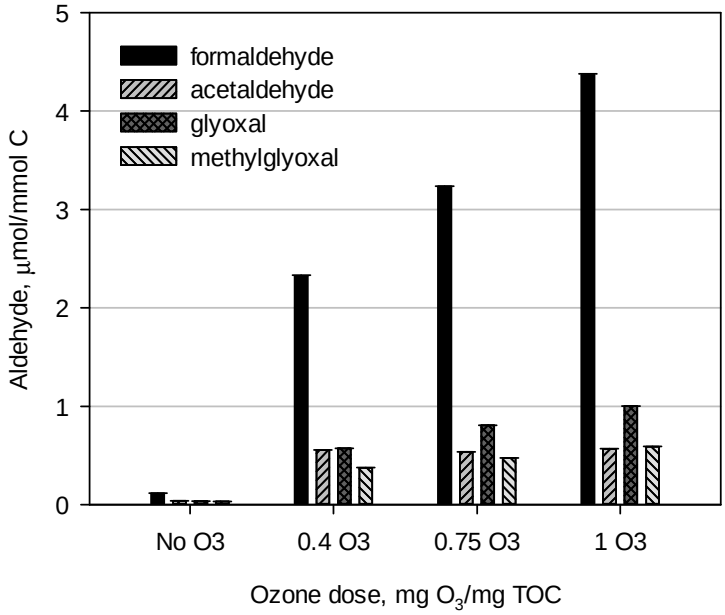

124

125 Figure S7. Aldehyde formation as a function of ozone dose.

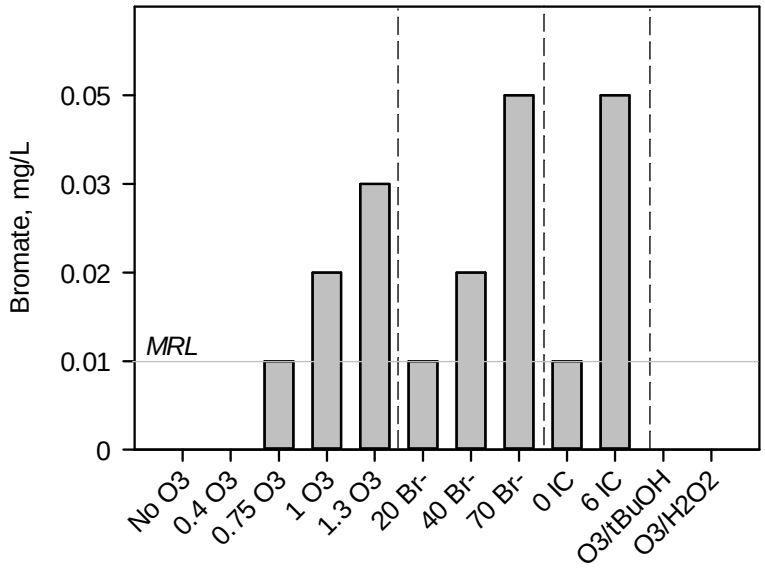

126

127 Figure S8. Bromate concentrations at different transferred ozone dose (0 – 1.3 mg/mg TOC),
128 bromide concentrations (20 – 70 μg/mg TOC), inorganic carbon (IC) concentrations (0 – 6 mg/mg
129 TOC), and in the presence of t-BuOH (10 mM) and H_2O_2 (1 mg/mg O_3). Baseline conditions: TOC =
130 18 mg/L as C, pH = 7 (1 mM phosphate), temperature = 22±1 ^{0}C, bromide = 20 μg/mg TOC, IC = 0
131 mg/mg TOC, transferred ozone dose = 0.75 mg/mg TOC. Bromide and IC concentrations were
132 varied by spiking NaBr and $NaHCO_3$, respectively. *MRL* = method reporting limit.

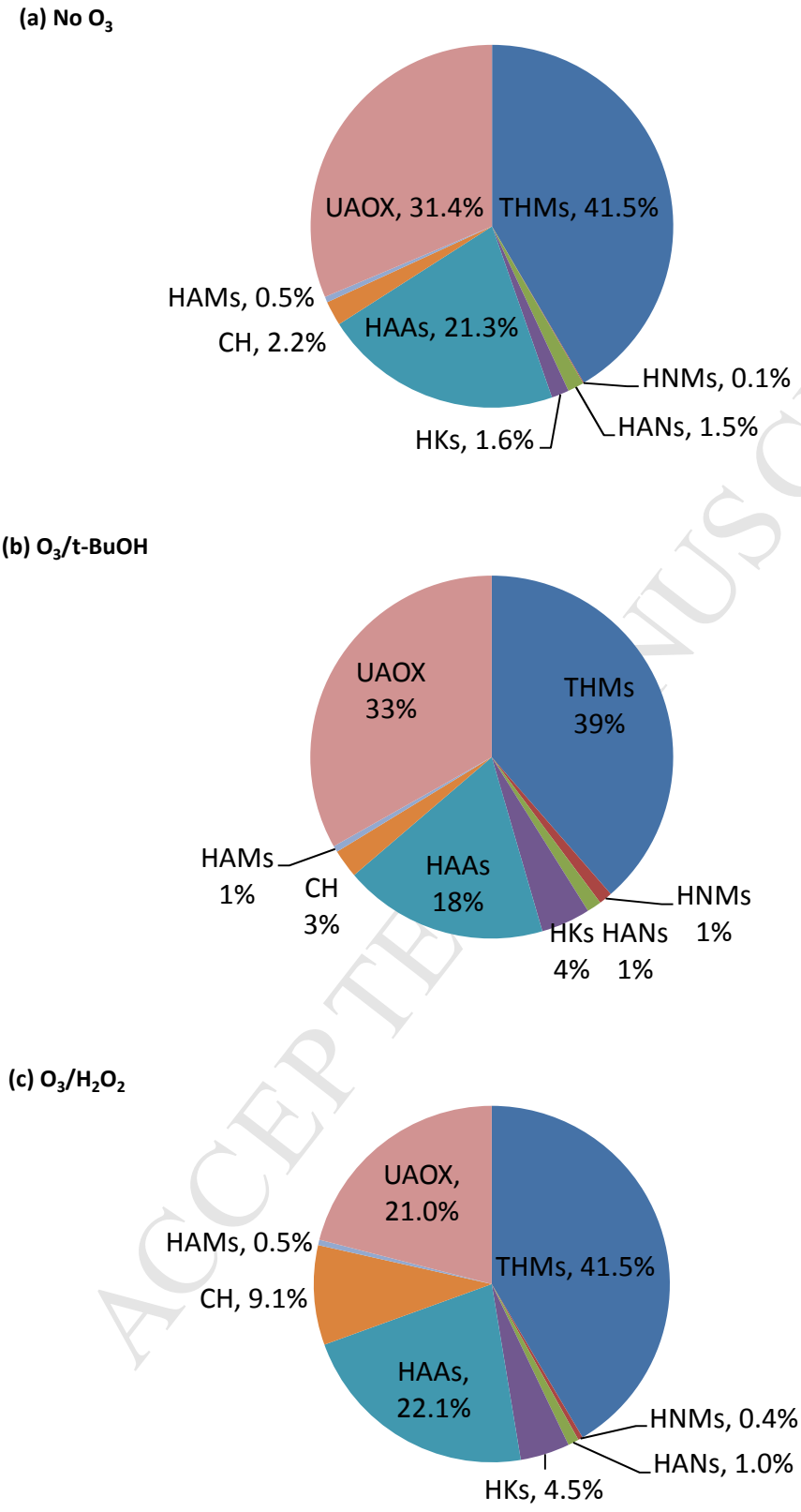

Figure S9. Comparison of AOX distribution for samples treated with (a) no O_3, (b) O_3/t-BuOH, and (c) O_3/H_2O_2.

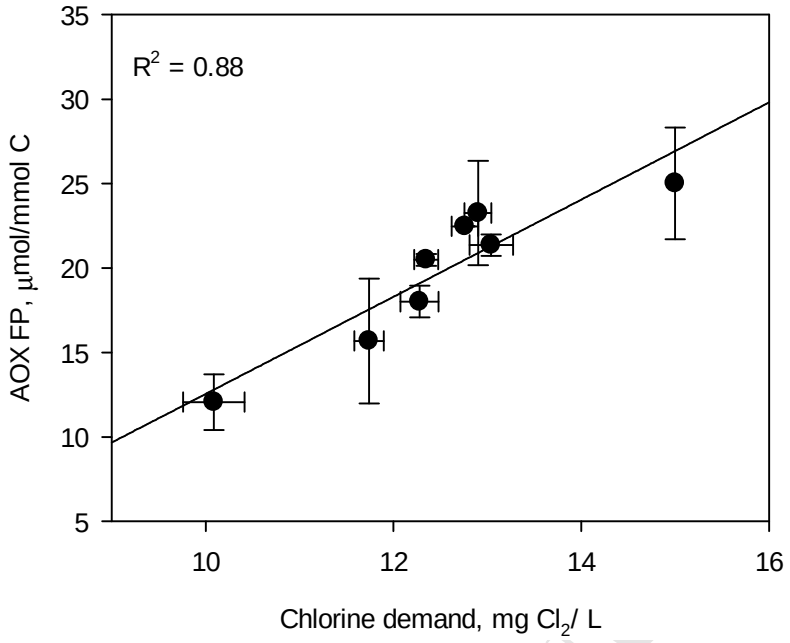

138

139 Figure S10. Linear relationship of AOX formation potential (AOXFP) with chlorine demand

140

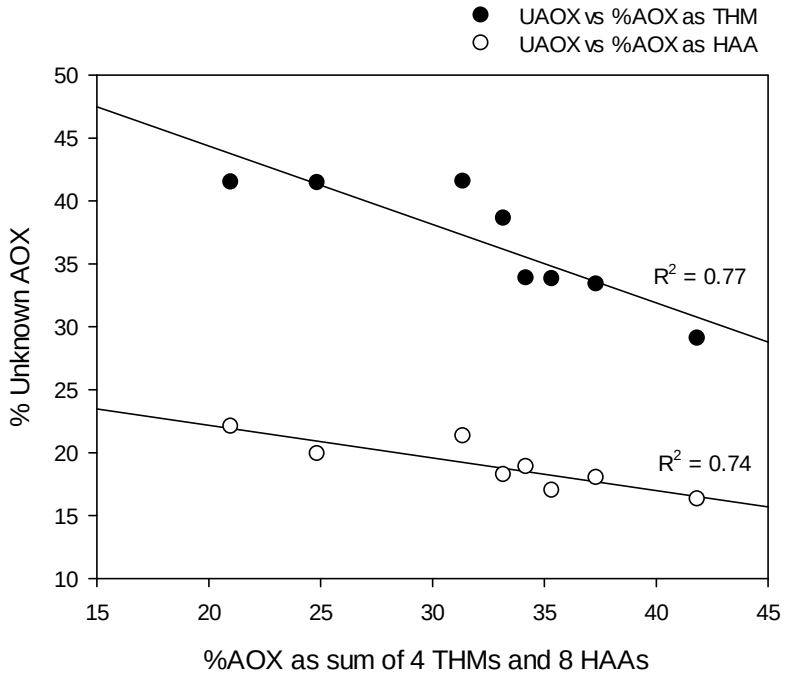

141

142 Figure S11. Dependence of unknown AOX on %AOX accounted for by THMs and HAAs

143

144

145 **References**

146

147 Chen, Q., Westerhoff, P., Leenheer, J.A. and Booksh, K. (2003) Fluorescence excitation-emission
148 matrix regional integration to quantify spectra for dissolved organic matter. Environ. Sci.
149 Technol. 37, 5701-5710.
150 Elovitz, M.S. and von Gunten, U. (1999) Hydroxyl radical/ozone ratios during ozonation processes.
151 I. the Rct concept. Ozone-Sci. Eng. 21(3), 239-260.
152 Farre, M.J., Day, S., Neale, P.A., Stalter, D., Tang, J.Y. and Escher, B.I. (2013) Bioanalytical and
153 chemical assessment of the disinfection by-product formation potential: role of organic matter.
154 Water Res. 47(14), 5409-5421.
155 Gjessing, E.T., Egeberg, P.K. and Hakedal, J. (1999) Natural organicmatter in drinking water - the
156 "NOM-typing project", background and basic characteristics of original water samples and NOM
157 isolates. Environ. Int. 25(2/3), 145-159.
158 Liu, W., Andrews, S.A., Stefan, M.I. and Bolton, J.R. (2003) Optimal methods for quenching H_2O_2
159 residuals prior to UFC testing. Water Res. 37(15), 3697-3703.
160 Munch, J.W., Munch, D.J. and Winslow, S.D. (1998) Method 556: Determination of crabonyl
161 compounds in drinking water by pentafluorobenzylhydroxylamine derivatization and capillary gas
162 chromatography with electron capture detection. US EPA, Cincinnati, OH, USA.
163 Sun, L., Perdue, E.M. and McCarthy, J.F. (1995) Using reverse osmosis to obtain organic matter
164 from surface and ground waters. Water Res. 29(6), 1471-1477.
165 Yeh, R.Y., Farre, M.J., Stalter, D., Tang, J.Y., Molendijk, J. and Escher, B.I. (2014) Bioanalytical
166 and chemical evaluation of disinfection by-products in swimming pool water. Water Res. 59, 172-
167 184.

168

169